Bulletin of Engineering Geology and the Environment (2024) 83:204
https://doi.org/10.1007/s10064-024-03680-3

ORIGINAL PAPER

# Application of Sentinel-1 InSAR to monitor tailings dams and predict geotechnical instability: practical considerations based on case study insights

Nahyan M. Rana[1,2] · Keith B. Delaney[1] · Stephen G. Evans[1] · Evan Deane[3] · Andy Small[4] · Daniel A. M. Adria[5] · Scott McDougall[6] · Negar Ghahramani[7] · W. Andy Take[8]

Received: 18 October 2023 / Accepted: 7 April 2024 / Published online: 29 April 2024


## Abstract

Tailings storage facilities (TSFs) impound mining waste behind dams to ensure public safety, but failure incidents have prompted calls for more robust monitoring programs. Satellite-based interferometric synthetic aperture radar (InSAR) has grown in popularity due to its ability to remotely detect millimeter-scale displacements in most urban and some natural terrains. However, there remains a limited understanding of whether InSAR can be as accurate or representative as on-the-ground instruments, whether failures can be predicted in advance using InSAR, and what variables govern the quality and reliability of InSAR results. To address these gaps, we analyze open-source, medium-resolution Sentinel-1 data to undertake a ground-truth assessment at a test site and a forensic analysis of five failure cases. We use a commercial software with an automated Persistent Scatterer (PS) workflow (SARScape Analytics) for all case study sites except one and a proprietary algorithm (SqueeSAR) with a dual PS and Distributed Scatterer (DS) algorithm for the ground-truth site and one forensic case. The main goal is to deliver practical insights regarding the influence of algorithm/satellite selection, environmental conditions, site activity, coherence thresholds, satellite-dam geometry, and failure modes. We conclude that Sentinel-1 InSAR can serve as a hazard-screening tool to help guide where to undertake targeted investigations; however, most potential failure modes may not exhibit InSAR-detectable accelerations that could assist with time-of-failure prediction in real time. As such, long-term monitoring programs should ideally be integrated with a combination of remote sensing and field instrumentation to best support engineering practice and judgment.

**Keywords** Tailings storage facility · Dam safety · Mining hazards · Remote sensing · Failure prediction · Risk management

✉ Nahyan M. Rana
nrana@klohn.com

1 Department of Earth and Environmental Sciences, University of Waterloo, Waterloo, ON N2L3G1, Canada

2 Klohn Crippen Berger, Toronto, ON M5H 1T1, Canada

3 BGC Engineering, Edmonton, AB T5J 4A1, Canada

4 Klohn Crippen Berger, Fredericton, NB E3B 2L2, Canada

5 Knight Piésold, Vancouver, BC V6C 2T8, Canada

6 Department of Earth, Ocean and Atmospheric Sciences, The University of British Columbia, Vancouver, BC V6T 1Z4, Canada

7 WSP, Lakewood, CO 80228, USA

8 Department of Civil Engineering, Queen's University, Kingston, ON K7L 3N6, Canada

## Introduction

### Preamble

Tailings storage facilities (TSFs) impound fine-grained, wet, often geochemically hazardous mine waste behind constructed dams in perpetuity for societal and environmental protection (Vick 1983; Blight 2010). TSFs can store considerable volumes of flowable material that, if released accidentally, could produce far-reaching and long-lasting consequences, as evidenced by a number of TSF failure incidents in recent years (e.g., Morgenstern et al. 2015, 2016; Robertson et al. 2019; Rana et al. 2021). Such events highlight the importance of implementing proactive monitoring systems at TSF sites to ensure safe performance.

A key objective in TSF monitoring is to observe for potential signs of instability by analyzing spatiotemporal

rates of displacement—a variable that is of special concern in scenarios involving creep deformation, static liquefaction, or foundation deformations. In industry practice, the displacement rate has conventionally been monitored by field observations, in-situ instrumentation (e.g., monitoring prisms, inclinometers, and extensometers), ground-based InSAR, ground-based or airborne Light Detection and Ranging (LiDAR), and/or photogrammetry. Another available technique is satellite InSAR, which has been utilized as a complementary, and potentially cost-effective, monitoring tool in mining practice (Hu et al. 2017; Raspini et al. 2022). The central focus of this article is on the utility of satellite InSAR for monitoring tailings dams and predicting instability.

By conducting interferometric analysis of SAR satellite images, one can measure millimeter-scale displacements in the line-of-sight (LOS) direction of the satellite or in two dimensions (east–west horizontal and up-down vertical) if two satellite orbit tracks in opposite directions are overlapping spatially and temporally (e.g., Hu et al. 2017; Mazzanti et al. 2021). The Sentinel-1 satellite, commenced in mid-2015 by the European Space Agency (ESA), has become a popular SAR sensor in displacement monitoring studies due to the open-source data release and the revisit times of 6 or 12 days in most of the world.

Among the numerous InSAR deformation analysis techniques (Aswathi et al. 2022), Persistent Scatterer (PS) is able to produce highly precise, long-term displacement time-series mainly for human-built structures such as bridges, roads, buildings, and dams (Ferretti et al. 2001; Crosetto et al. 2016). Small Baseline Subset (SBAS) InSAR is an alternative time-series approach that was designed to improve the spatial distribution and density of "Distributed Scatterer" (DS) observation points in vegetated study areas, albeit at reduced spatial resolution (Berardino et al. 2002; Casu et al. 2006).

A technical drawback of InSAR is the complicated and lengthy workflow that necessitates the use of computers and software with high data processing capacity. This obstacle, along with the conceptual complexity of advanced InSAR, has contributed to a limited archive of case studies on tailings dams. Hu et al. (2017) monitored displacements at the Kennecott TSF in the USA by integrating ENVISAT, ALOS Palsar-1, and Sentinel-1A data. Mazzanti et al. (2021) used over 400 Sentinel-1 images in the ascending and descending orbit direction to study displacements at the Zelazny Most TSF in Poland.

To date, three recent TSF breach cases have been forensically analyzed using InSAR: 2018 Cadia, Australia (Carla et al. 2019a; Jefferies et al. 2019; Thomas et al. 2019; Hudson et al. 2021; Bayaraa et al. 2022), 2019 Feijao, Brazil (Gama et al. 2020; Holden et al. 2020; Rotta et al. 2020; Grebby et al. 2021), and 2022 Jiaokou, China (Duan et al. 2023; Su et al. 2024). The common conclusion in these case studies was that satellite InSAR can be an effective monitoring tool for TSFs exhibiting slow, long-term deformations, but awareness of limitations is needed as it relates to the oblique geometry of 1-D LOS displacement measurements, the difficulty in predicting instantaneous failure mechanisms, phase unwrapping errors, and loss of coherence. Mirmazloumi et al. (2023) also re-examined the Cadia and Feijao cases using a PS algorithm to test an early warning system based on machine learning.

While the Cadia case demonstrated a precursor acceleration phase that could have assisted in time-to-failure prediction (Carla et al. 2019a), such anomalous displacement patterns were not as readily apparent in the Feijao and Jiaokou cases. This leads to an incomplete understanding of whether tailings dam failures can indeed be predicted in advance using InSAR data alone or whether accurate InSAR-derived failure predictions can only be achieved only under certain criteria/conditions (e.g., processing algorithm, satellite-dam geometry, failure mechanism). To build on previous advancements, the case study inventory needs to be expanded in order to explore the capabilities and limitations of InSAR when monitoring tailings dams in diverse site conditions and with different potential failure modes.

## Goal and scope

Using Sentinel-1 data, this study helps address this research gap in two ways. First, we present a ground-truth assessment at a test site where InSAR results are compared to in-situ monitoring prism data. Second, we examine the precursor displacements in 5 TSF failure cases (2017–2019) selected from published databases (Islam and Murakami 2021; Rana et al. 2021, 2022) based on the following criteria: (i) their variability in reported failure mechanisms and site characteristics and (ii) the spatial–temporal coverage of Sentinel-1 data over the sites. Of the 5 failure events, 3 are new case studies whereas the 2 others (Cadia and Feijao) have already been analyzed using InSAR in preceding studies, which allows us to compare our findings versus published results.

In all of the cases, it was possible to retrieve only the 1-D LOS displacements—i.e., spatially and temporally overlapping ascending and descending orbit tracks, which allow insights into east–west and vertical displacements, were not available. To process the Sentinel-1 InSAR data, we used two software/algorithms: (i) for the ground-truth site and 4 of 5 forensic case studies, a commercial software (SARScape Analytics) that offers an automated workflow for PS analysis; and (ii) for the ground-truth site and only 1 forensic case study, the proprietary algorithm SqueeSAR which is integrated with an advanced PS + DS technique (Ferretti et al. 2011). The use of multiple processing techniques helped demonstrate how the quality of InSAR results

may vary depending on the adopted algorithm and the site conditions.

The ultimate goal of this study was to provide practical insights and considerations for engineers and mine owners who may be considering Sentinel-1 InSAR as a long-term monitoring tool for their TSFs. This goal is pursued by the following approach:

1. We analyze the accuracy of Sentinel-1 InSAR on a site-scale using multiple software/algorithms.
2. We assess if unstable locations and accelerations in precursor displacements can be detected by the present approach. This allows us to:
    a. Identify high-deformation hotspots to match with the observed breach location and reported breach mechanism, which is important for hazard assessment;
    b. Check if the failure was preceded by accelerating displacements, and if so, how many weeks in advance this trend was observed, which is important for risk management; and/or
    c. Identify errors in the results due to the inherent limitations of the selected software, the limitations of Sentinel-1 data, or the LOS velocity threshold being exceeded.
3. We comment on the influence of dam-satellite geometry, environmental conditions, and failure modes on the quality, value, and interpretation of LOS displacement results.

## Background and approach

### SAR data processing

Methods to process SAR data for displacement monitoring range from open-source software such as SNAP/SNAPHU (Chen and Zebker 2002), HyP3/MintPy (Yunjun et al. 2019) and EZ-InSAR (Hrysiewicz et al. 2023), to commercially available software such as GAMMA (Werner et al. 2000; Wang et al. 2020), SARPROZ (Perissin et al. 2011; Bakon et al. 2014), and SARScape (Gama et al. 2020), to company-specific proprietary algorithms such as APSIS (Sowter et al. 2016; Grebby et al. 2021) and SqueeSAR (Ferretti et al. 2011; Carla et al. 2019a; Bischoff et al. 2020). To our knowledge, there are no scientific studies to date that compare the effectiveness of different processing algorithms/software specifically for tailings dam monitoring applications.

For the present study, we used ENVI SARScape Analytics (v. 5.6), which was developed by SARMap and is commercially distributed by NV5 Geospatial (formerly L3Harris Geospatial), to process Sentinel-1 data for the ground-truth test site and 4 of 5 forensic case studies. The software offers a streamlined workflow for PS-InSAR analysis, whereby each processing step is automated and the analysis runtime is reduced substantially. The Analytics package is a condensed, limited version of the entire SARScape software suite, which has been previously used to analyze the 2019 Feijao TSF failure using both the PS and SBAS techniques (Gama et al. 2020). The steps that are automated in the PS processing chain include co-registration, interferogram creation, coherence generation, height estimation, baseline refinement, noise filtering, and phase unwrapping. For a technical background on the standard PS algorithm, we refer to Ferretti et al. (2001), Crosetto et al. (2016), and references therein.

We explored the feasibility of alternative software such as SNAP/SNAPHU and SARPROZ, but the balanced cost- and time-saving features of SARScape Analytics were deemed to be most convenient for the comprehensive scope of this study. However, there are inherent drawbacks in the automated approach of SARScape Analytics; it is not possible to produce or extract individual interferograms, to modify any parameters or steps in the workflow (except the coherence), and to view or modify the reference location.

We downloaded open-source Sentinel-1 Single Look Complex (SLC) Interferometric Wide (IW) scenes from the Alaska Satellite Facility (ASF) web platform. Other input variables into the SARScape Analytics software were the geoid type (EGM2008), the base global digital elevation model (DEM) which we selected to be 30-m resolution SRTM-3 v4, and the area of interest in KML format (must be between 4 and 25 $km^2$).

For the ground-truth site and one forensic case study (2018 Cieneguita, Mexico), the Sentinel-1 images were also processed using the SqueeSAR algorithm (Ferretti et al. 2011). The SqueeSAR processing was performed by TRE Altamira based on instructions on the study area and time-series duration provided by the lead author (N. Rana). SqueeSAR overcomes the limitations of alternative software packages by integrating both PS and DS points during analysis, thus enhancing the spatial density of point-cloud displacement data in most terrains. SqueeSAR has been used to study tailings dam failures (2018 Cadia, Australia), open-pit slope instabilities (e.g., Carla et al. 2019a), urban deformation (e.g., Bischoff et al. 2017, 2020), and natural landslides (e.g., Carla et al. 2019a,b) and is best-suited to monitor displacement rates of < 1000 mm/year. The technical framework of SqueeSAR is described in Ferretti et al. (2011).

The comparison between SARScape Analytics and SqueeSAR in the ground-truth assessment is not intended to be a competition, but rather to demonstrate how the quality of InSAR results can differ depending on the adopted data processing technique, which is ultimately of practical value to engineers and mine owners.

For 3 case study sites, we filtered the PS data based on a minimum coherence of 0.70, whereas for the 2 sites where environmental conditions affected InSAR data availability, we reduced the minimum coherence to 0.57–0.65. Our thresholds are higher than the 0.45 value applied in the ISBAS analysis of Feijao by Grebby et al. (2021) and are comparable to the minimum temporal coherence of 0.60 adopted by Mazzanti et al. (2021) in their PS analysis of Zelazsny Most TSF.

## Ground-truth assessment

As a complementary lead-up to the forensic case studies, we undertook a ground-truth assessment at a tailings dam situated in a cold-climate setting. Key identifier details of the mine and TSF are kept confidential to adhere to the non-disclosure agreement signed with the mine owner. We compared Sentinel-1B PS-InSAR LOS cumulative displacement results to in-situ data captured via two monitoring prisms (MP5 and MP3) over the same study period. The MPs were installed in late 2018 along the tailings dam. MP5 is at the crest while MP3 is on the downstream slope, and both are located at the SE corner of the dam. The average accuracy of the MP horizontal and vertical displacement measurements is approximately ± 10 mm. The errors are mainly due to setup error of the total station, and the magnitude of the errors varies depending on how far the prism is located from the setup location.

The MP data indicates that this section of the dam crest has exhibited some settlement deformation mainly toward the upstream (western) direction, whereas the downstream (east-facing) slope of the dam has shown relatively stable behavior with minimal cumulative movement. The main objective here was to check if Sentinel-1 InSAR, as processed via both SARScape Analytics and SqueeSAR, shows reasonable consistency with the MP data and can adequately represent a tailings dam experiencing displacement rates between 0 and 50 mm/year.

The Sentinel-1B track used for analysis had an ascending (i.e., roughly south-to-north) orbit geometry and a LOS incidence angle of 31°. The tailings dam trends north–south, whereby the downstream slope of the dam faces eastward away from the satellite but is still exposed at an acute angle to the satellite's LOS. On SARScape Analytics, we processed 36 Sentinel-1B images from May 2019 to October 2021, excluding the winter months from the processing stack because snow/ice is known to reduce the coherence of InSAR observations (Carla et al. 2019b; Kim et al. 2022). The SqueeSAR processing involved a total of 42 Sentinel-1B images over roughly the same study duration, also excluding the winter images. We confirmed the start and end dates of the winter months by checking for snow/ice cover on the TSF on high-resolution, high-frequency RapidEye and PlanetScope satellite imagery for the site.

To facilitate a fair time-series comparison, we followed these steps:

1. The original MP datasets included results collected during the winter months, whereas Sentinel-1 images corresponding to winter months were excluded from the InSAR processing stack. To avoid temporal inconsistency, we baselined the cumulative displacement results from the Sentinel-1 and MP datasets to the start of the Spring season in each study year—that is, our time-series comparisons encompass the Spring-Fall seasons of 2019–2021.
2. The MP data was originally reported as horizontal-easting and vertical. To avoid geometric inconsistency, we converted/projected the MP data to the Sentinel-1 LOS (31° eastward) using the following formula: *LOS-projected displacement = vertical displacement * cos(31°) − horizontal-easting displacement * sin(31°).*
3. For the comparisons, we selected the InSAR data point closest to the corresponding MP. The comparisons were quantitatively assessed by calculating average differences in the displacement measurements between the different time-series datasets, as well as via the root mean square error (RMSE) calculated by the formula: $\sqrt{\frac{1}{n}\sum_{i=1}^{n}(d_A - d_B)^2}$, where $d_A$ and $d_B$ represent displacements from InSAR or MP data and $n$ is number of comparison observations.

## Forensic case studies

This section describes the approach to investigating the precursor LOS displacements in 5 tailings dams that experienced a breach in the period 2017–2019. The cases are listed in Table 1. We selected these cases after screening databases of TSF failures (e.g., Islam and Murakami 2021; Rana et al. 2021, 2022) based on two criteria. First, the cases encompass a variety of breach mechanisms, allowing us to check for distinct displacement patterns depending on the failure mechanism (e.g., internal erosion vs. liquefaction vs. subsidence). Second, the 5 cases occurred in 5 countries with diverse climatic, topographic, and land-use regimes. This allows us to check for environmental conditions that influence the quality and reliability of the InSAR results.

For some of the cases, the predisposal variables (i.e., the underlying causal variables that preconditioned the precarious stability of the TSF), trigger mechanisms (i.e., a natural or anthropogenic activity that caused the breach to occur at a particular location at a given time), and failure modes (i.e., the mechanism by which the breach and outflow occurred) are poorly described in existing literature. These underlying

**Table 1** TSF failure cases analyzed in this study by Sentinel-1 InSAR, including the assigned qualitative levels of knowledge uncertainty for each case based on our literature review of the corresponding predisposal variables, trigger mechanisms, and failure modes (see definitions in text). Background details for these cases are provided throughout "Forensic case studies"

| TSF failure | Country | Site location (Lat, Long) | Failure date (Y-M-D) | Knowledge uncertainty | | |
|---|---|---|---|---|---|---|
| | | | | Predisposal variables | Trigger mechanism | Failure mode |
| Tonglvshan | China | 30.08, 114.95 | 2017–3-12 | Medium | High | Low |
| Cadia | Australia | − 33.5, 148.99 | 2018–3-9 | Low | Low | Low |
| Cieneguita | Mexico | 27.12, − 108.03 | 2018–6-4 | Medium | High | Medium |
| Feijao | Brazil | − 20.12, − 44.12 | 2019–1-25 | Low | Low | Low |
| Hindalco | India | 23.36, 85.86 | 2019–4-9 | Medium | High | High |

factors form the background story of each case; therefore, our knowledge of these factors has an influence on our judgment of the InSAR results. In Table 1, we assign qualitative levels of knowledge uncertainty for each case:

- "High uncertainty" means that the factor is virtually unknown due to lack of research.
- "Medium uncertainty" means that there are news articles or satellite images that provide basic information on, or insights into, the factor.
- "Low uncertainty" means that the factor has been well-documented in scientific material.

Details on the Sentinel-1 image processing stacks for each case are provided in Table 2. All of the cases were processed using SARScape Analytics with the exception of Cieneguita which was processed using SqueeSAR due to the highly vegetated environment. Our main objective was to forensically check whether the breach location and breach timing could have been predicted in advance using Sentinel-1 InSAR. For each case study, we adopted the following consistent approach:

1. We presented the LOS velocity map illustrating the calculated mean displacement rates per annum across the site.
2. We identified hotspots of detected movements in the unstable section and, where applicable, in other sections of the dam exhibiting similar detected behavior.
3. We plotted the cumulative LOS displacement time-series for these hotspot locations.
4. We checked if accelerations in the time-series could be observed.

Where precursor identifiers on the breach location and/or timing were not found, we provided explanations on the basis of the failure mechanism (if this information was available), the limitations of the processing algorithm, and/or the limitations of medium-resolution Sentinel-1 data. Out of our 5 case studies, only Cadia and Feijao have been forensically studied using InSAR (Carla et al. 2019a; Thomas et al. 2019; Gama et al. 2020; Rotta et al. 2020; Holden et al. 2020; Grebby et al. 2021; Hudson et al. 2021; Bayaraa et al. 2022), which allows us to compare our findings versus previously published results and comment on how different InSAR processing approaches influence the outcomes.

## Results

### Ground-truth assessment

Figure 1 shows the LOS velocity maps (i.e., calculated mean displacement rate per annum) from SARScape Analytics and SqueeSAR, enabling a side-by-side visual comparison. Both sets of InSAR data are filtered to show only points with coherence of 0.70 or greater. Figure 1 also includes a cross-sectional diagram to elucidate the geometric relationship between the satellite, the dam, and the MPs. The absence of InSAR data points in the TSF impoundment is due to surface wetness, indicating the presence of tailings or free water.

An important distinction is apparent between the two sets of InSAR data: the point density. Figure 2 shows that SqueeSAR produced 9876 data points over the TSF (the extent shown in Fig. 2A, B) whereas SARScape Analytics produced 4368. InSAR data coverage along the embankment was sparse, particularly for SARScape Analytics. This is attributed to (i) the inherent differences in the PS vs. PS + DS algorithms, (ii) on-site activity that likely reduced the stability of InSAR pixels, and/or (iii) the removal of winter images which could have contributed to loss of coherence and, consequently, loss of PS data for SARScape Analytics. The standard deviation in the SqueeSAR data was 5.5 mm/year compared to 6.2 mm/year for SARScape Analytics. Figure 2 also shows contrasting statistical distributions for the InSAR data when sorted by coherence; for SqueeSAR, the number of data points increases with increasing coherence,

**Table 2** Characteristics of the Sentinel-1 data acquired for each forensic case study. SARScape Analytics was used to process the InSAR data for all cases except Cieneguita, for which SqueeSAR was used

| TSF failure | SAR mission (band) | Product type | Beam mode | Orbit and look direction | Orbit track ID | Revisit time | Incidence line-of-sight (LOS) angle | Polarization | Time-series duration | No. of SAR images |
|---|---|---|---|---|---|---|---|---|---|---|
| Tonglvshan | Sentinel-1A/B (C-band) | Single Look Complex (SLC) | Interferometric Wide (IW) | Ascending (looking E-NE) | 40 | 12 days | 33.8° | VV + VH | 2015–06-05 to 2017–03-02 (21 months) | 49 |
| Cadia | | | | Descending (looking W-NW) | 45 | | 35.3° | | 2016–09-27 to 2018–02-25 (17 months) | 45 |
| Cieneguita | | | | | 56 | | 33.5° | | 2017–03-03 to 2018–06-02 (15 months) | 39 |
| Feijao | | | | | 53 and 155 | | 32.5° and 45° | | 2017–06-13 to 2019–01-22 and 2017–06-08 to 2019–01-17 (19 months) | 50 |
| Hindalco | | | | | 121 | | 38.2° | | 2017–09-04 to 2019–03-22 (18.5 months) | 52 |

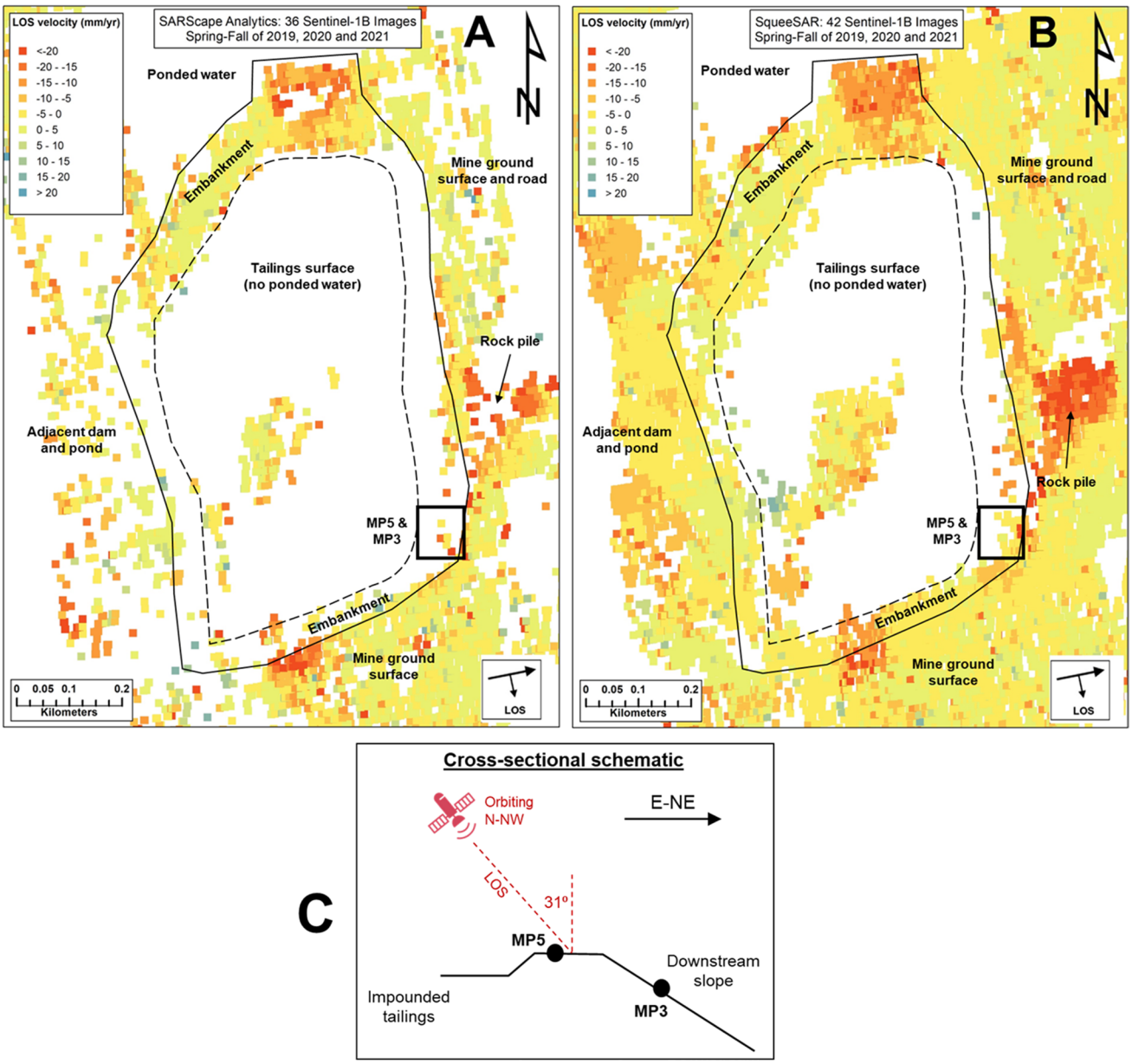


**Fig. 1** Sentinel-1 InSAR line-of-sight (LOS) velocity maps of the anonymized ground-truth TSF test site based on **A** SARScape Analytics and **B** SqueeSAR. Both sets of InSAR data are filtered to show only points with a coherence of ≥ 0.70. The maps are annotated with the locations of the selected monitoring prisms (MPs), the surface of the exposed tailings (dashed outline), the embankment (solid outline), the mine ground surface, ponded water sites, and the adjacent dam. Negative (red) values indicate detected movements away from the satellite whereas positive (blue) values indicate detected movements toward the satellite. **C** Cross-sectional schematic illustrating the geometric relationship between the satellite, the tailings dam, and the MPs

which is opposite to that of SARScape Analytics. As such, the mean coherence of SqueeSAR data was greater, implying a higher measurement precision on average.

Figure 3 presents the cumulative LOS displacement time-series for the two InSAR datasets and the two MP datasets on the dam crest and downstream slope for the Spring-Fall seasons of 2019–2021. The standard deviation of incremental displacements in the SARScape Analytics dataset was calculated to be 3.6 mm, marginally greater than the standard deviation of 3.0 mm for SqueeSAR. In comparison, as stated earlier, the accuracy for the MP data at this site was approximately ± 10 mm.

Table 3 presents statistical comparisons between these datasets. For the dam crest, the average differences ranged from 2.8 to 3.7 mm when comparing SARScape Analytics versus SqueeSAR results, from 4.4 to 5.0 mm when

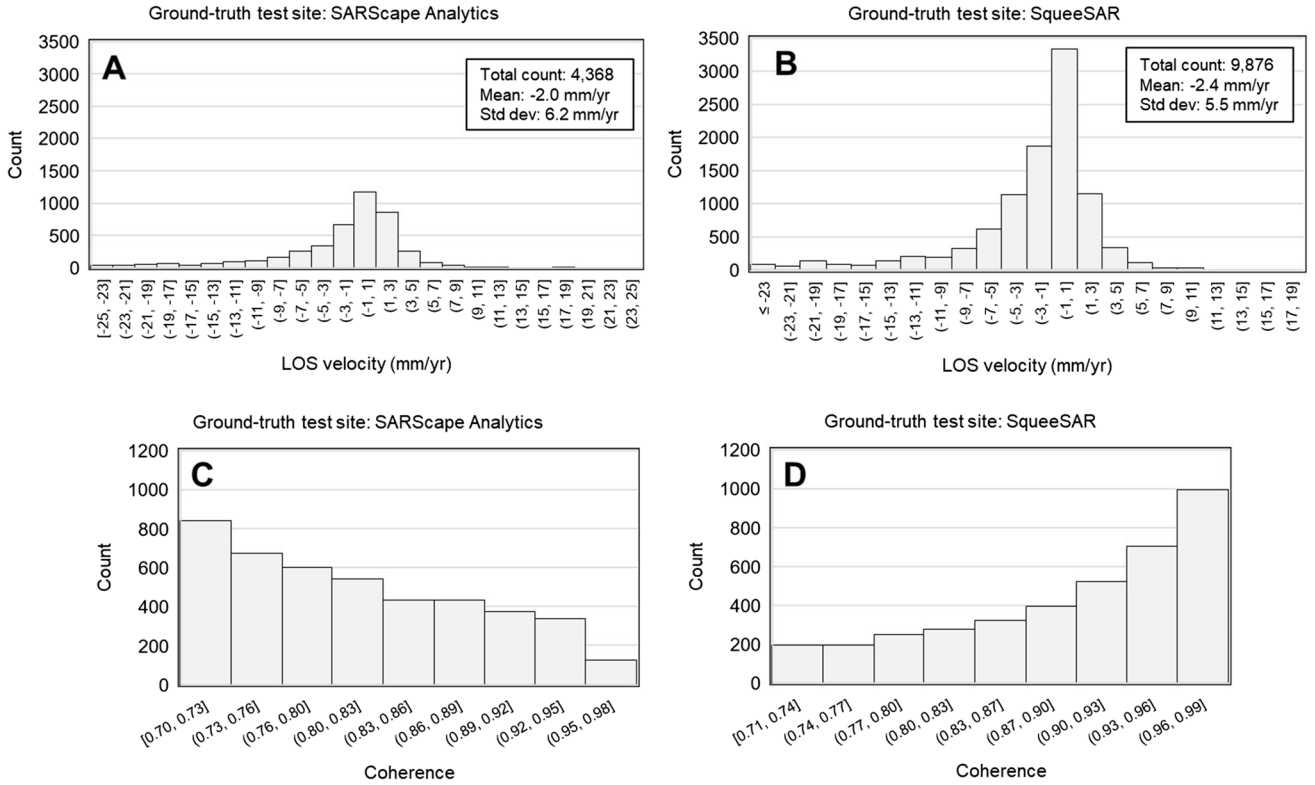


**Fig. 2** Comparisons of **A, B** line-of-sight (LOS) velocities (mm/year) and **C, D** coherence values between SARScape Analytics and SqueeSAR results for the ground-truth test site

comparing SARScape Analytics versus MP5 data, and from 2.4 to 5.0 mm when comparing SqueeSAR versus MP5. The RMSE values ranged from 3.6 to 6.0 mm (SARScape Analytics vs. SqueeSAR), 5.1 to 6.6 mm (SARScape Analytics vs. MP5), and 3.1 to 6.7 mm (SqueeSAR vs. MP5). For the downstream slope, the ranges of average differences were 1.5–6.0, 3.0–3.6, and 3.4–5.1 mm, respectively, and the ranges of RMSE values were 1.8–7.1, 3.7–4.1, and 4.4–6.1 mm, respectively.

Our results indicate that, at this particular tailings dam, Sentinel-1 InSAR was able to reasonably represent the displacement rates (all below 50 mm/year) on both the dam crest and downstream slope within a maximum RMSE of 7 mm. However, the loss or sparsity of InSAR data points along the dam crest due to on-site activity and the removal of winter images precluded us from performing additional comparisons to other MPs that are installed along the dam. This issue could be of concern to mine owners using InSAR to monitor tailings dams in cold-climate regimes or highly active TSFs undergoing tailings deposition and dam raises.

## Forensic case studies

This section presents the InSAR results for each forensic case study. The presentation of the InSAR results is preceded by a background review of the reported failure description. For all of the cases except Tonglvshan, we constructed time-lapse videos using between 60 and 120 PlanetScope (3 m resolution) optical satellite images to show the evolution of the TSFs until their breach. The open-access URL links to these time-lapse videos are listed in Table 4 in the Appendix.

### 2017 Tonglvshan, China

The Tonglvshan copper-iron TSF is located near Daye City in Hubei Province, China. On 12 March 2017, the northern section of the tailings dam experienced a breach with an approximate geometry of about 50 m breadth × 250 m width × 12 m height (Fig. 4). The released volume was reportedly ~ 500,000 $m^3$ (Zhuang et al. 2022) with an inundation area of 300,000 $m^2$ (Ghahramani et al. 2020). The failure reportedly occurred due to the long-term effects of weathering and gravity in the roof granite in the mine goaf underneath the TSF (Zhuang et al. 2022). This caused the upper strata to fail, which led to the subsidence and brittle instability in the dam foundation. The incident led to 2 deaths and 6 injuries (Zhuang et al. 2022).

Figure 5 shows the results from our analysis of 49 Sentinel-1 images over a duration of 21 months. The satellite had an ascending orbit parallel to the length of the TSF with

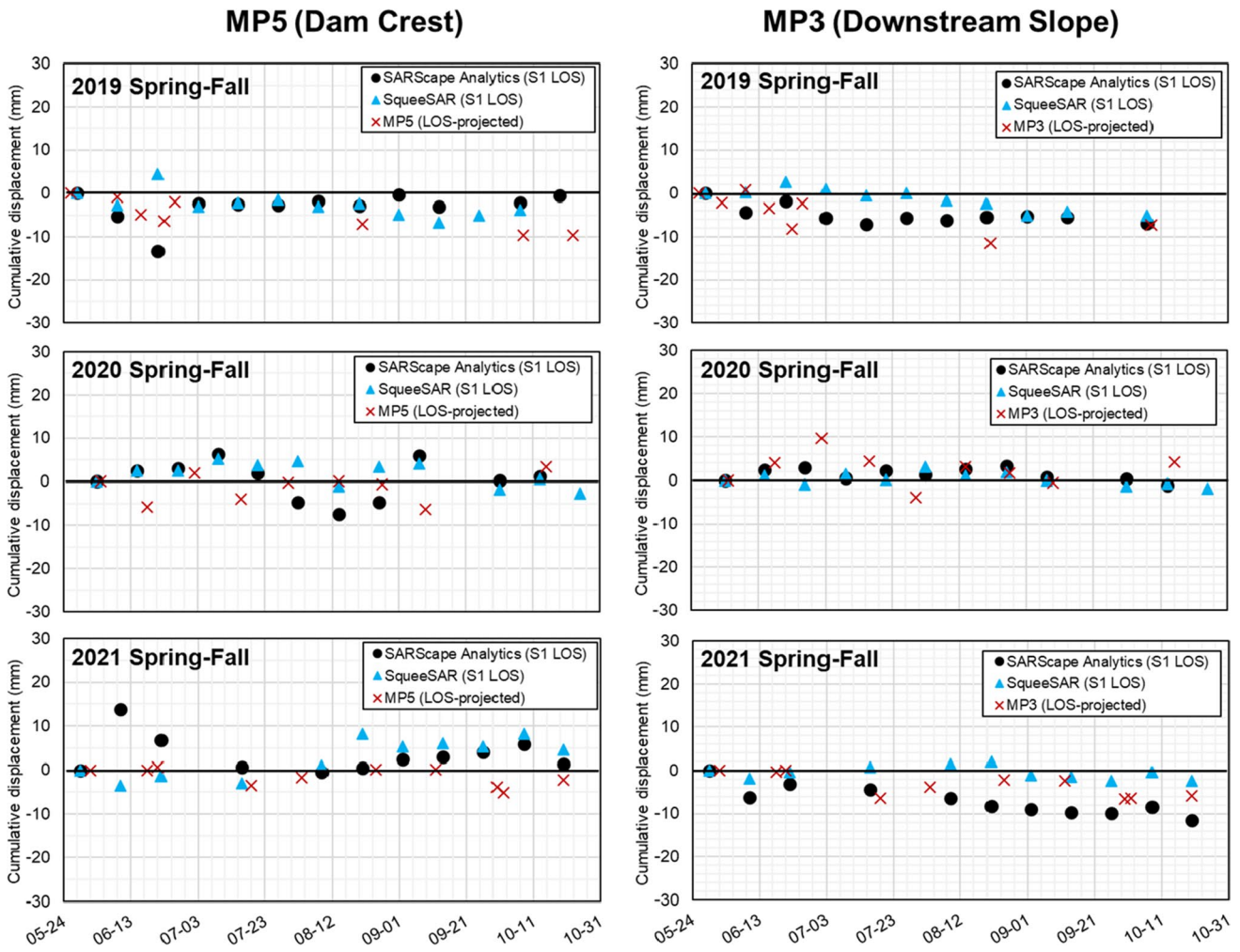


**Fig. 3** Ground-truth results comparing the Sentinel-1 line-of-sight (LOS) InSAR cumulative displacement data (processed on SARScape Analytics and SqueeSAR) to in-situ cumulative displacement data from monitoring prisms MP5, on the crest, and MP3, on the downstream slope, of the tailings dam. The study period encompasses the Spring-Fall seasons of 2019–2021 (i.e., winter images were excluded from the processing stack), with all sets of data being baselined to the start of each Spring-Fall study period

a LOS incidence angle of 33.8° toward E-NE. This implies that, at the northern section that experienced the breach, displacements in the downstream (N-NW) direction were along-track in relation to the satellite orbit (Fig. 5B) and thus were poorly captured. However, LOS components of vertical, settlement- and subsidence-related deformation can be measured.

The LOS velocities in the infrastructure surrounding the TSF were generally close to 0 mm/year (i.e., stable). This contrasts with the deformation regime along the tailings dam, sections of which were experiencing anomalously high LOS velocities: only a single data point at the northern section that eventually breached and a few data points at the middle of the western wall that remained stable. As shown in the time-series (Fig. 5C), the LOS deformation patterns were similar in both locations, suggesting a near-constant rate of movement away from the satellite (i.e., settlement and potential subsidence activity) with a total displacement of ~ 50 mm over the study duration, but there was no discernible evidence of precursor acceleration at any section along the tailings dam.

However, it is worth reiterating that the unstable northern section was geometrically unfavorable in relation to the satellite's LOS compared to the western wall that was directly facing the LOS. Moreover, given the loss of coherence, a few isolated data points are not sufficient to study the instability of a tailings dam with confidence. These issues inevitably influence our interpretation of the results for this case.

### 2018 Cadia, Australia

The Cadia gold mine in New South Wales, Australia, operates two large TSFs: the Northern TSF (NTSF) and the Southern TSF (STSF), both of which are

**Table 3** Statistical comparisons of cumulative line-of-sight displacements in terms of average differences and root mean square error (RMSE) between SARScape Analytics (SSA), SqueeSAR (SQ), and monitoring prism (MP) data for the dam crest and downstream (DS) slope of the ground-truth TSF site (see Fig. 3 for the time-series plots)

| Study period | Average difference (mm) for dam crest | | | Average difference (mm) for DS slope | | | RMSE (mm) for dam crest | | | RMSE (mm) for DS slope | | |
|---|---|---|---|---|---|---|---|---|---|---|---|---|
| | SSA vs. SQ | SSA vs. MP5 | SQ vs. MP5 | SSA vs. SQ | SSA vs. MP3 | SQ vs. MP3 | SSA vs. SQ | SSA vs. MP5 | SQ vs. MP5 | SSA vs. SQ | SSA vs. MP3 | SQ vs. MP3 |
| Spring-Fall 2019 | 3.3 | 5.0 | 2.4 | 4.3 | 3.0 | 5.1 | 6.0 | 6.3 | 3.1 | 4.6 | 3.7 | 6.1 |
| Spring-Fall 2020 | 2.8 | 4.4 | 4.1 | 1.5 | 3.6 | 3.4 | 4.4 | 5.1 | 4.7 | 1.8 | 4.1 | 4.6 |
| Spring-Fall 2021 | 3.7 | 4.4 | 5.0 | 6.0 | 3.4 | 3.8 | 3.6 | 6.6 | 6.7 | 7.1 | 3.8 | 4.4 |

upstream-constructed, stepped side-hill impoundments (Jefferies et al. 2019). In March 2018, ~ 300 m long section of the SW section experienced failure in the NTSF (Fig. 6). We created a time-lapse video of the Cadia dam using 120 PlanetScope images between September 2016 and September 2018 (Table 4). The video shows that the failure process was two-staged: the initial breach occurred on 9 March 2018, and another secondary event occurred at the same location on 11 March 2018. Jefferies et al. (2019) identified the main failure cause to be a low-density, highly compressible Forest Reef Volcanics (FRV) layer in the foundation underneath the SW wall of the NTSF. This previously unidentified unit was strain-weakening—that is, the unit became brittle when subjected to high loads. Accelerated displacements over this foundation unit triggered static liquefaction in the loose, saturated tailings in the NTSF. The Cadia failure has been forensically examined by InSAR using proprietary processing software in several publications (Carla et al. 2019a; Jefferies et al. 2019; Thomas et al. 2019; Hudson et al. 2021; Bayaraa et al. 2022). These studies identified accelerating deformation in the 2–3 months preceding the dam collapse.

Figure 7 shows our PS-InSAR results after processing 45 Sentinel-1 images over a 17-month duration. The satellite had a descending orbit track with a LOS incidence angle of 35°. Although the unstable dam face was obliquely exposed to the satellite's LOS, the LOS components of vertical settlements along the dam were well-captured. The LOS velocity patterns showed that the vicinity of the unstable section, especially along the dam crest, represented a hotspot of anomalously high movements (Fig. 7A). These observations resemble those seen in previous publications on the Cadia event, whereby the time-series (Fig. 7C) shows the commencement of the acceleration phase in January 2018. However, there appear to be errors associated with the final two data points leading up to the failure. We observed a similar time-series pattern for all of the other high-velocity data points along the breach section. This issue may be caused by phase unwrapping errors due to exceedance of the maximum LOS velocity threshold of 28 mm over a 12-day revisit time, as previously suggested by Bayaraa et al. (2022). However, these errors were not observed in Carla et al. (2019a) who used SqueeSAR and in Jefferies et al. (2019) who used the SBAS algorithm within the complete SARScape software package. Jefferies et al. (2019) also stated that SBAS is more appropriate to capture strong, nonlinear accelerations. As such, the issue encountered here appears to reflect a key technical limitation of PS-InSAR when monitoring relatively fast, accelerating deformations, with major implications for the ability to make time-of-failure predictions.

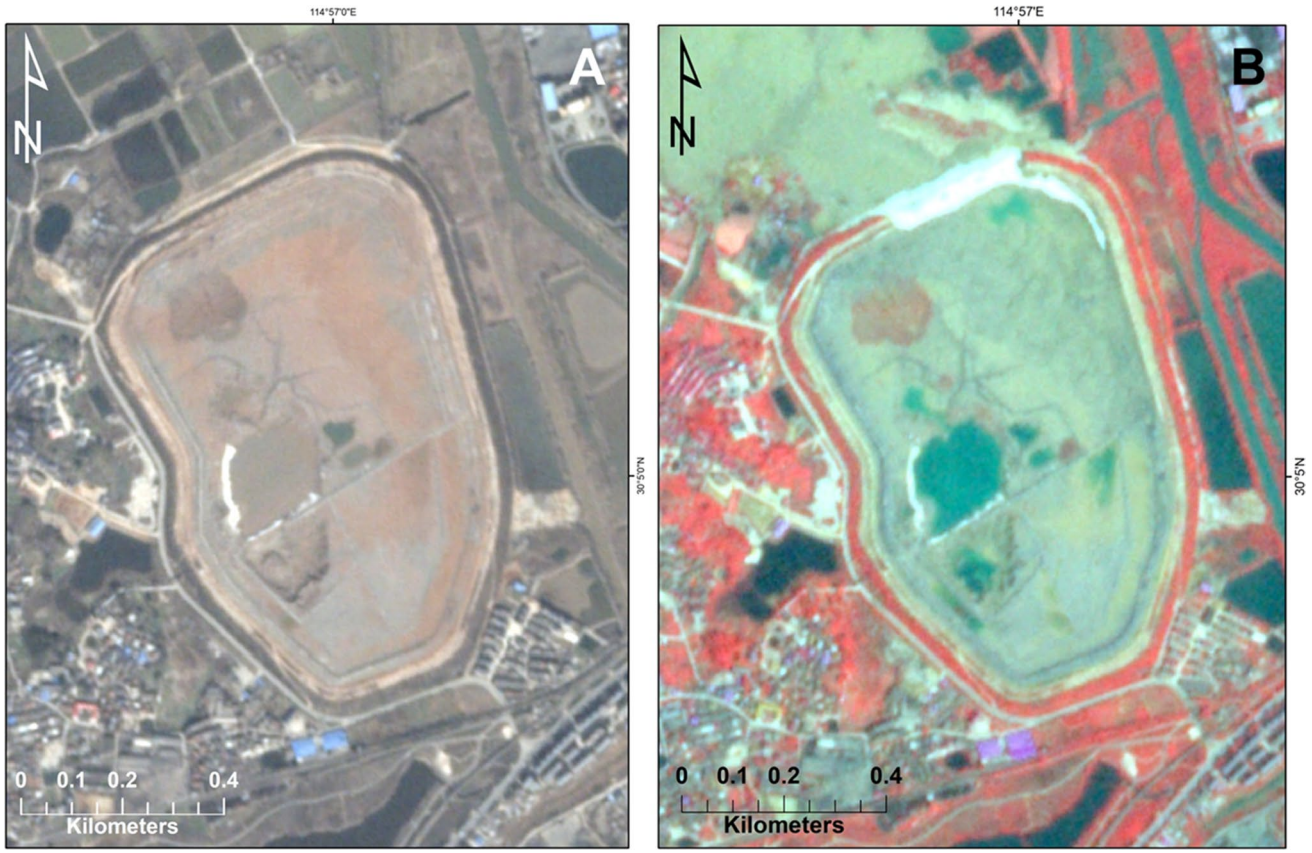


**Fig. 4** **A** Pre-failure (13 February 2017) and **B** post-failure (13 April 2017) PlanetScope (3 m resolution) images of the 12 March 2017 Tonglvshan tailings dam breach in China

### 2018 Cieneguita, Mexico

The Cieneguita gold-silver tailings dam in Chihuahua, Mexico, was breached on 4 June 2018 (Fig. 8). The total released volume was ~ 440,000 $m^3$, including ~ 250,000 $m^3$ of tailings and ~ 190,000 $m^3$ of embankment and construction materials (Rana et al. 2021 2022). According to historical satellite imagery on Google Earth, the tailings deposition commenced at this site in mid-2013. The TSF size was relatively small, covering an area of ~ 35,000 $m^2$ with a dam crest length of about 150 m around the date of failure. According to local reports, premonitory signs included extensive cracking along the downstream face of the dam about 4 months prior to failure, likely indicative of ongoing internal erosion and a weakened state of the embankment in response to rapid loading on the sloping impoundment (Rana et al. 2021 2022). At least three mine workers were killed by the collapse. The tailings flow caused at least three fatalities and achieved a runout distance of 15 km along Canitas Creek (Ghahramani et al. 2020). We constructed a time-lapse video of the Cieneguita TSF using 60 PlanetScope images spanning the period January 2017 to July 2018 (Table 4). The video shows that the TSF was undergoing rapid depositional and construction activity.

SARScape Analytics was found to be ineffective in producing reliable InSAR results due to the forested terrain at this site. As such, SqueeSAR was used to process 39 Sentinel-1 images encompassing the 15-month study period, as shown in Fig. 9. The SqueeSAR results still showed a complete absence of data points along the central (breached) portion of the embankment, mainly due to the construction activity. We observed three high-velocity (< − 20 mm/year) data points at the left edge/corner of the dam slope and plotted the average cumulative displacement time-series in Fig. 9C. The total displacement recorded here was ~ 40 mm, without evidence of precursor acceleration. In this time-series, we also detected a "cyclic" pattern of displacements from September 2017 onwards. This pattern could be a reflection of on-site activity rather than geotechnical processes in the dam itself. However, it remains difficult to confirm this given the lack of knowledge on site-specific conditions and activities over the study period.

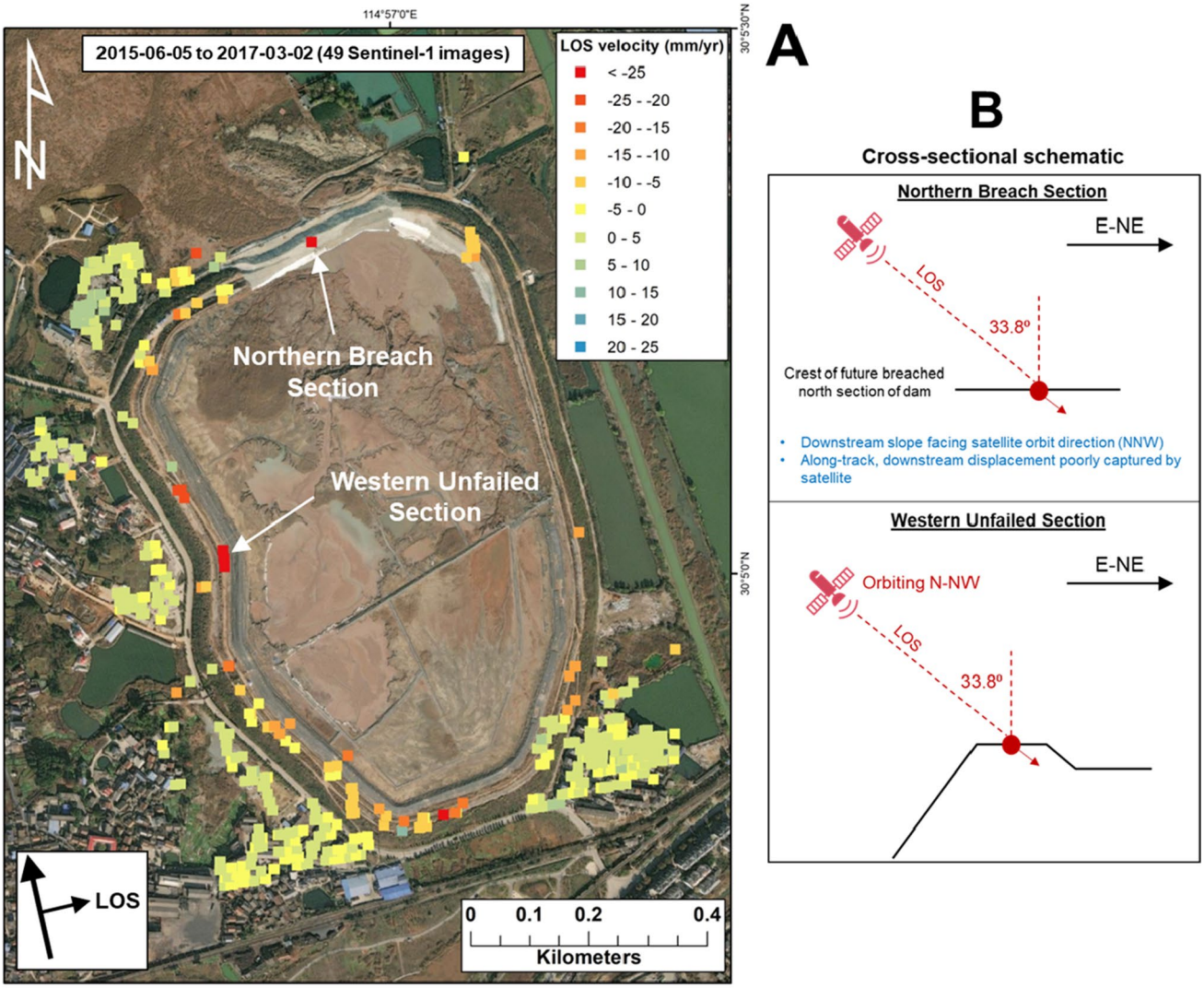
A
114°57'0"E
30°5'30"N
30°5'0"N
2015-06-05 to 2017-03-02 (49 Sentinel-1 images)
LOS velocity (mm/yr)
< -25
-25 - -20
-20 - -15
-15 - -10
-10 - -5
-5 - 0
0 - 5
5 - 10
10 - 15
15 - 20
20 - 25
Northern Breach Section
Western Unfailed Section
LOS
0 0.1 0.2 0.4
Kilometers
B
Cross-sectional schematic
Northern Breach Section
E-NE
LOS
33.8°
Crest of future breached north section of dam
Downstream slope facing satellite orbit direction (NNW)
Along-track, downstream displacement poorly captured by satellite
Western Unfailed Section
E-NE
Orbiting N-NW
LOS
33.8°

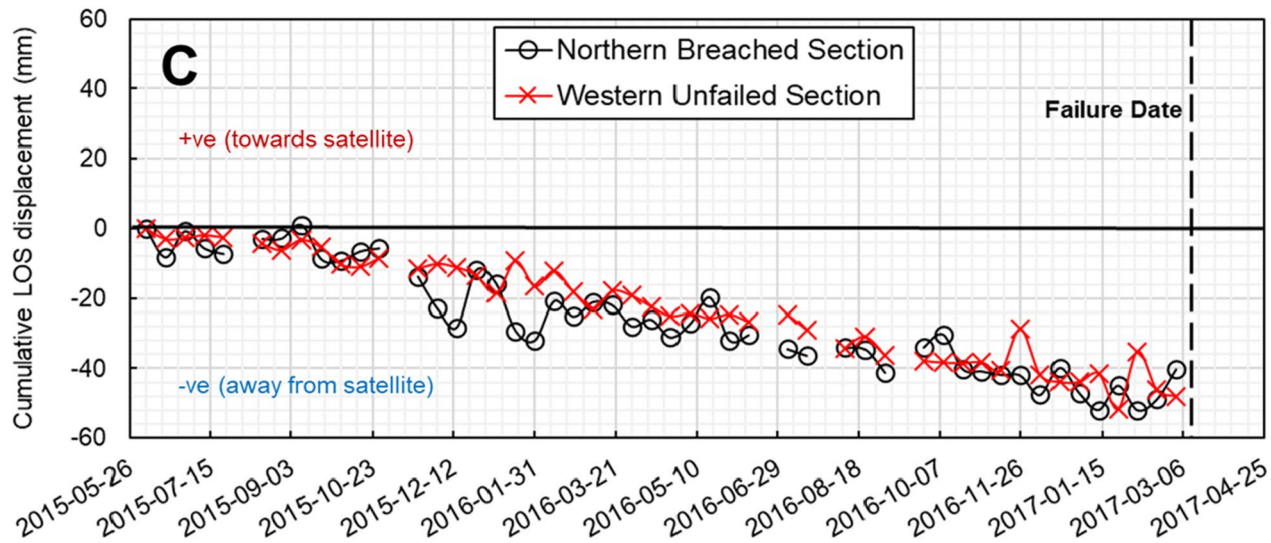
C
Northern Breached Section
Western Unfailed Section
Failure Date
+ve (towards satellite)
-ve (away from satellite)
Cumulative LOS displacement (mm)
60
40
20
0
-20
-40
-60
2015-05-26
2015-07-15
2015-09-03
2015-10-23
2015-12-12
2016-01-31
2016-03-21
2016-05-10
2016-06-29
2016-08-18
2016-10-07
2016-11-26
2017-01-15
2017-03-06
2017-04-25

◂**Fig. 5** Sentinel-1 PS-InSAR results, processed on SARScape Analytics with a minimum coherence of 0.57, for the 12 March 2017 Tonglvshan TSF breach in China. **A** Line-of-sight (LOS) velocity map, annotated with the northern breach section (1 data point) and western unfailed section (average of 5 data points) selected for time-series analysis. Negative (red) values indicate detected movements away from the satellite, positive (blue) values indicate detected movements toward the satellite, and green-yellow values indicate detected stable areas. **B** Cross-sectional schematics for the two sections illustrating the geometric relationship between the satellite, the tailings dam, and the PS points selected for time-series analysis (arrow indicates direction of InSAR-detected LOS movement). **C** Cumulative LOS displacements over the time-series duration for the two sections

### 2019 Feijao, Brazil

The Feijao TSF is located near Brumadinho, Brazil. The dam collapsed on 25 January 2019, releasing 9.7 M $m^3$ of tailings, equivalent to 75% of the total impounded volume (Fig. 10). The failure was predisposed by several factors (Robertson et al. 2019): (i) the application of the upstream raise method with a steep slope; (ii) the deposition of fine, weak tailings near the crest of the dam; (iii) a setback in construction, which caused the upper portions of the dam to overlie weaker, finer-grained tailings; (iv) the lack of effective horizontal drainage, groundwater seepage, and high rainfall that led to high internal water levels; (v) a loss of suction in the unsaturated portion of the tailings, leading to a sudden loss of strength; and (vi) high iron content in the tailings resulting in particle bonding via iron oxidation, causing brittle behavior in the tailings. These issues preconditioned the occurrence of static liquefaction on the date of failure, likely triggered by drilling activity on a metastable section of the dam (Arroyo and Gens 2021; Arenas et al. 2023). The resulting tailings flow resulted in 272 deaths and rendered long-lasting environmental and socio-economic effects in the region, prompting major updates to global industry standards in tailings management (Global Tailings Review 2020). We constructed a time-lapse video of the Feijao TSF using 90 PlanetScope satellite images between June 2017 and February 2019 (Table 4), which confirm that the TSF was in an inactive state during this period.

A number of previous studies have presented InSAR investigations of the Feijao event (Gama et al. 2020; Holden et al. 2020; Grebby et al. 2021; Mirmazloumi et al. 2023). The differences in data interpretation and conclusions between these studies are summarized as follows:

- Gama et al. (2020) used the SBAS and PS algorithms in SARScape (the complete software, not the automated and limited Analytics package that is used in this study) to process 26 Sentinel-1 images and detected a mild acceleration phase in the weeks preceding the collapse. The authors concluded that their confidence in their inverse-velocity prediction results was low due to the wide error distributions that were not centered around the actual failure date.
- Holden et al. (2020) from 3vGeomatics Inc. used proprietary software to analyze Sentinel-1 (> 3 years of images over two orbit tracks), TerraSAR-X (~ 2 years of images), and COSMO-SkyMed data (30 images) and concluded that the precursor acceleration was not statistically significant or anomalous enough to have been a reliable warning sign. They used the findings of Robertson et al. (2019), who noted "no apparent signs of distress prior to failure," as a geotechnical justification for this conclusion.
- Grebby et al. (2021) processed 45 Sentinel-1 images from two satellite orbit tracks (both descending) using the ISBAS algorithm in the Punnet (now APSIS) software (Terra Motion Limited). Based on their inverse-velocity analysis of 4–5 data points that showed a prediction interval of ~ 40 days around the failure date, the authors concluded that the collapse was foreseeable.
- Mirmazloumi et al. (2023) used a PS algorithm implemented in the Geomatics Division of the Centre Tecnològic de Telecomunicacions de Catalunya (CTTC) in Spain (Devanthery et al. 2014). They processed 68 Sentinel-1 images with the goal of testing a machine learning-based early warning system. The time-of-failure forecast capability for Feijao was found to have some promise albeit with the requirement of expert interpretation due to the low PS point density, given the forested landscape.

Figure 11 shows our PS results from the processing of 50 Sentinel-1 images over two orbit tracks (155 and 53, both descending) over a 19-month duration. Track 155 has a relatively high LOS incidence angle (45°) compared to Track 53 (32.5°) (Fig. 11D). This implies that the PS results of Track 53 are more sensitive to vertical deformations, whereas Track 155 results are more sensitive to sub-horizontal displacements. The dam face was exposed to the satellite's LOS at an oblique angle (Fig. 11D); this makes it a non-ideal geometry to estimate the rate of movement in the downstream direction, which is almost parallel to the orbit track. It is worth noting that, by implementing a high coherence threshold (0.70) via the PS analysis on SARScape Analytics, there were no data points detected along the dam toe. A similar issue was encountered by Mirmazloumi et al. (2023), though their selected coherence threshold was not reported.

The time-series results from both orbit tracks corresponding to the dam crest, shown in Fig. 11E, show that the LOS cumulative displacements were in the order of 40 mm (away from the sensor) over the 19-month duration. This compares to averages of 27 mm (SBAS) and 35 mm (PS) over a 10-month duration reported by Gama et al. (2020), an average of 20 mm (ISBAS) over 17 months reported by Grebby et al. (2021), and

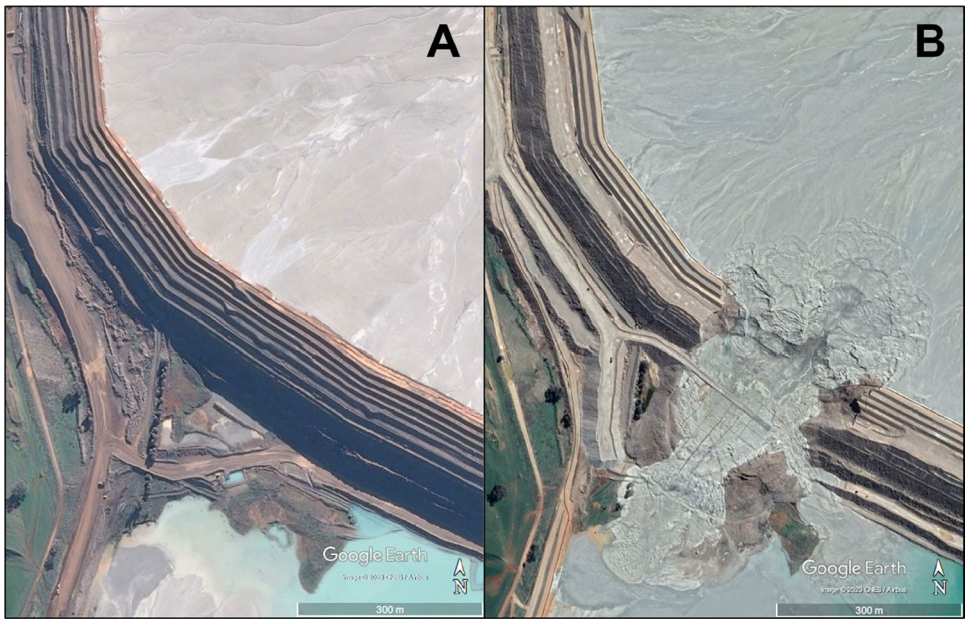


**Fig. 6** **A** Pre-failure (11 June 2016) and **B** post-failure (12 September 2018) Google Earth Worldview-2 (0.5 m resolution) images of the 9 March 2018 Cadia tailings dam breach in Australia

averages of 40 mm (Track 53) and 60 mm (Track 155) over 27 months reported by Holden et al. (2020). None of our InSAR data points present any visually discernible evidence of precursor accelerations. Our conclusion is, therefore, consistent with that of Holden et al. (2020)—i.e., although the dam was experiencing deformations, the failure date could not have been predicted in advance using InSAR data alone.

#### 2019 Hindalco, India

Hindalco Industries operates a bauxite residue TSF near the village of Muri in Jharkhand, India. The TSF covers a surface area of ~ 300,000 $m^2$ and was dammed by ~ 5 m high gabion retaining walls with a perimeter of over 2 km. Historical satellite images on Google Earth show that a water pond covered the SW portion of the impoundment for several years until sometime in the period 2011–2014, when tailings were deposited into the pond. There were also two water storage ponds as distinct compartments in the TSF.

On 9 April 2019, about 600 m of the SW section of the gabion wall was breached (Fig. 12). The failed materials comprised the entire extent of the former pond area, as well as one of the water storage ponds. The flowslide was bounded by railway tracks toward the west and travelled for a few hundred meters southward along the margin of the tracks toward the village. The trigger mechanism of the event is unclear, but local reports have pointed to the poorly constructed gabion wall as a failure cause and to a potential undrained failure mechanism based on field observations, eyewitness accounts, and analysis of a publicly available video of the breach area (Kumar 2019; Rana et al. 2021). We created a time-lapse video of the Hindalco TSF using 120 PlanetScope images captured over the period September 2017 to September 2019 (Table 4).

Figure 13 shows the PS-InSAR results for the Hindalco case. We processed 52 Sentinel-1 images spanning 18.5 months. The satellite was on a descending orbit track with a LOS angle of 38.2°. Along the section of the gabion wall that breached (i.e., on the west and south side), the crest was exposed to the satellite's LOS whereas the wall slopes were partly or completely hidden. For the generation of cumulative displacement time-series, we selected the PS points that exhibited the highest LOS velocities. In both the western and southern failed sections, these data points indicated a LOS cumulative displacement of ~ 40 mm over the study duration, without any notable indication of precursor accelerations.

## Discussion

Our analyses show that the quality or value of Sentinel-1 InSAR results for a tailings dam may be influenced by several variables and considerations with practical implications for monitoring accuracy and failure predictions. At the same time, we acknowledge that the methodology underpinning this study consisted of some limitations and user judgment, and future research will require overcoming these limitations to build on our comprehensive work. All of these discussion points are presented in the following sub-sections.

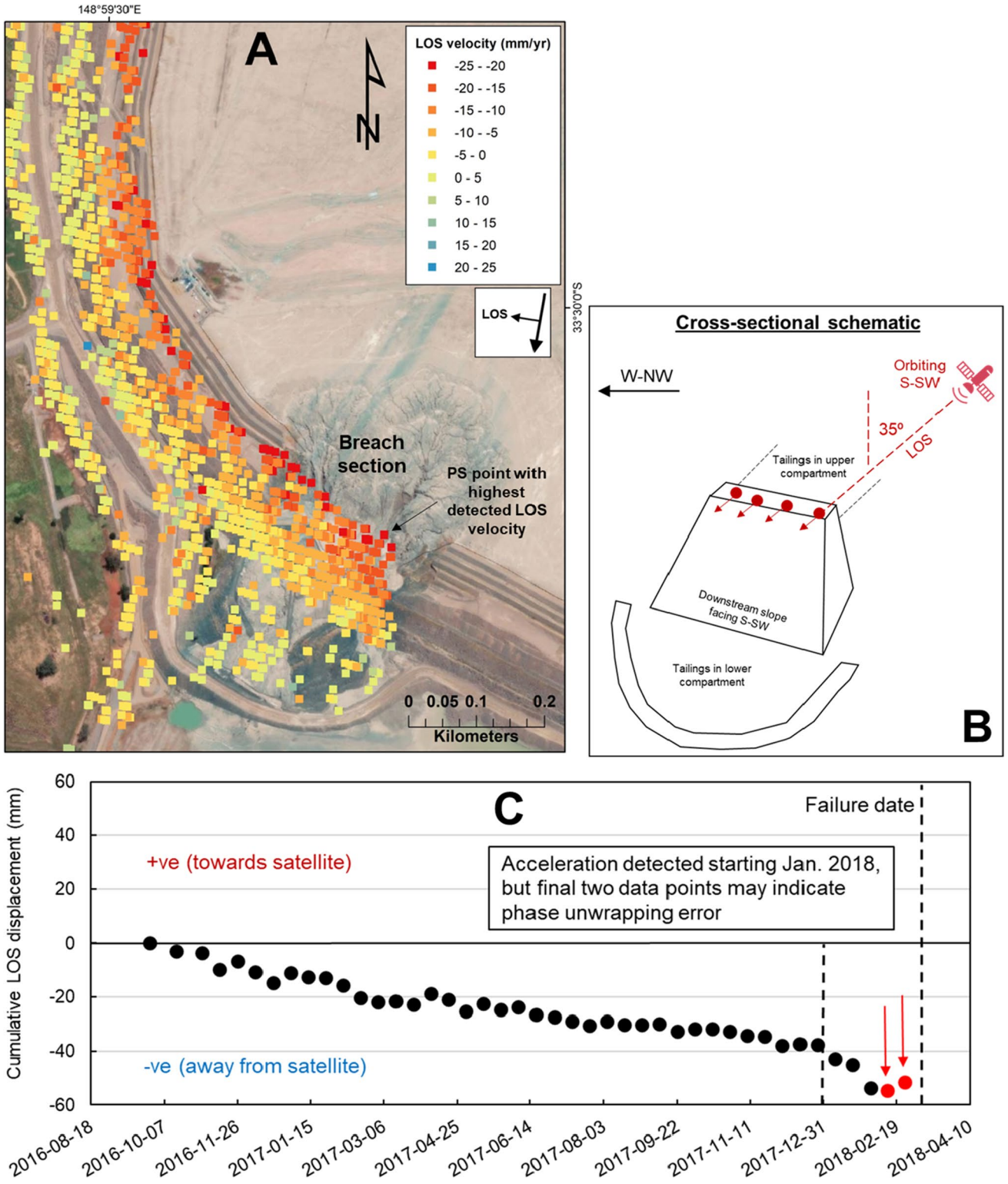


**Fig. 7** Sentinel-1 PS-InSAR results, processed on SARScape Analytics, for the 9 March 2018 Cadia TSF breach in Australia. **A** Line-of-sight (LOS) velocity map, annotated with the breach location and the PS point selected for time-series analysis. Negative (red) values indicate detected movements away from the satellite, positive (blue) values indicate detected movements toward the satellite, and green-yellow values indicate detected stable areas. **B** Cross-sectional schematic illustrating the geometric relationship between the satellite, the tailings dam, and the PS points. The small red arrows indicate the direction of LOS movement, in this case away from the satellite. **C** Cumulative LOS displacement time-series for the data point at the center of the breach section that exhibited the highest detected LOS velocity (− 25 mm/year)

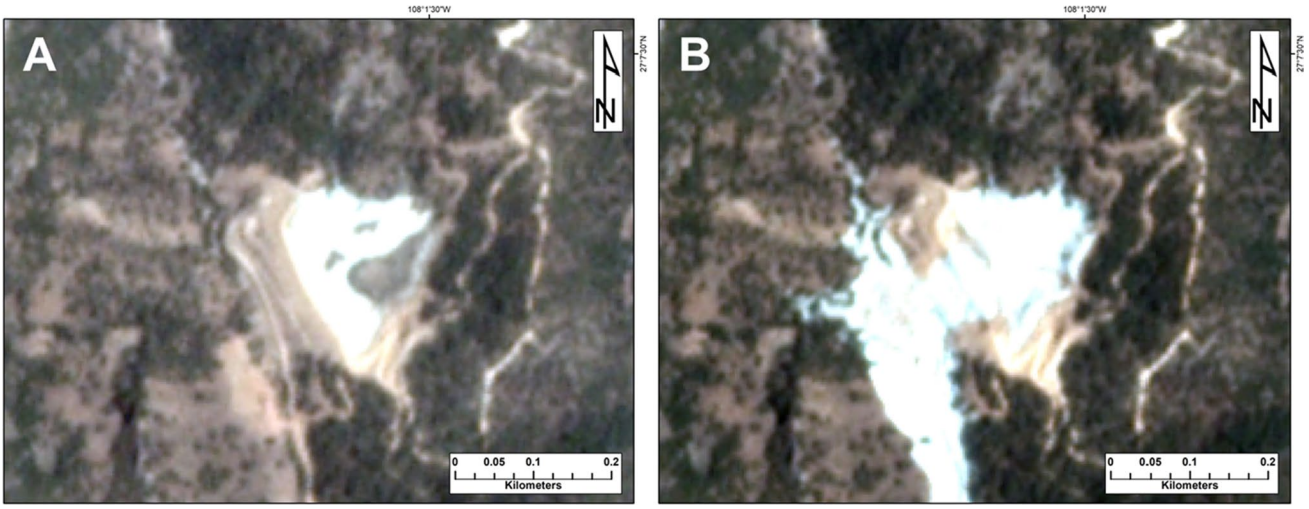


**Fig. 8** **A** Pre-failure (3 June 2018) and **B** post-failure (5 June 2018) PlanetScope (3 m resolution) images of the 4 June 2018 Cieneguita tailings dam breach in Mexico

## Practical considerations

### Environmental conditions

It is well-established that C-band InSAR data (e.g., Sentinel-1) and the PS technique are not well-suited to monitor areas with dense vegetation. This is due to the average wavelength of C-band data (~6 cm) that prevents signal penetration through wooded or forested sites, as well as the temporal de-correlation that often characterizes such sites (e.g., Crosetto et al. 2010). Therefore, this approach would be ineffective for monitoring most of the thousands of tailings dams in sub-tropical regions such as Brazil, China, India, and Mexico. One way to overcome this limitation is to use L-band data (see "Selection of satellite data") and the SBAS algorithm to monitor TSFs in such regions.

Snow/ice cover also affects the quality of InSAR data, which necessitated the removal of winter images for our ground-truth test site. At the same time, removing a significant section of the processing stack leads to a long temporal baseline, which can cause phase unwrapping problems and underestimate real deformations (Pawluszek-Filipiak et al. 2023). Both conflicting issues can impact the monitoring performance of satellite InSAR for tailings dams in cold-climate regions (e.g., Canada, Nordic countries, Russia). A viable approach to bypass this limitation is to install artificial corner reflectors on tailings dams, which help concentrate InSAR measurements on select sections that require monitoring (Pawluszek-Filipiak et al. 2023).

### Dam orientation in relation to satellite line-of-sight (LOS)

The satellite orbit direction and the LOS angle have an important influence on the detected magnitude of InSAR displacement results and the subsequent data interpretation. This effect is particularly applicable to TSFs that consist of multiple dams of variable orientations. However, LOS components of vertical deformation on the dam crest can still be well-detected irrespective of the satellite orbit direction, as observed in the Cadia case. The tracking of vertical versus horizontal deformation (when using only a single satellite rather than multiple overlapping satellites) is sensitive to the satellite's LOS angle, whereby a smaller angle corresponds to a stronger sensitivity to vertical movements.

Where possible, the retrieval of 2-D InSAR data (vertical displacements and horizontal east–west displacements) is most ideal. However, a major existing limitation is that, due to the polar orbit of SAR satellites, sub-horizontal displacements in the north–south direction cannot be retrieved.

### Selection of satellite data

Given that Sentinel-1 is currently the only open-source SAR imagery with near-global coverage, it remains the most popular option for InSAR researchers over alternative data sources such as TerraSAR-X, SAOCOM-1, ALOS PALSAR-1/2, and COSMO-SkyMed. However, our research has shown that the limitations of Sentinel-1 may have implications for effective long-term monitoring of tailings dams.

For instance, when monitoring a smaller-sized TSF, the resolution of Sentinel-1 data (20 × 5 m) may be too coarse,

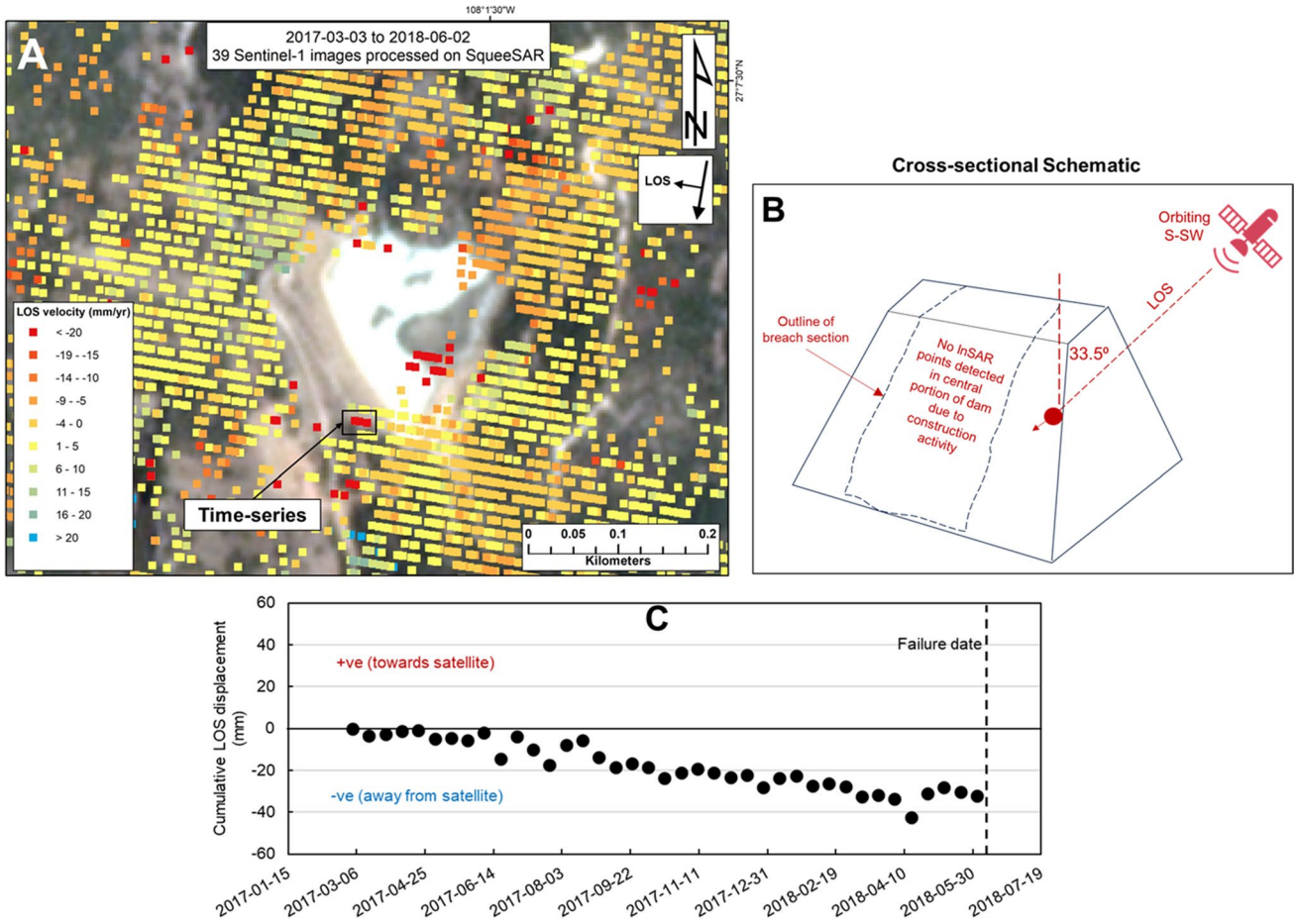


**Fig. 9** Sentinel-1 PS + DS InSAR results, processed on SqueeSAR with a minimum coherence threshold of 0.60, for the 4 June 2018 Cieneguita TSF failure in Mexico. **A** Line-of-sight (LOS) velocity map, annotated with the PS points selected for time-series analysis. Negative (red) values indicate detected movements away from the satellite, positive (blue) values indicate detected movements toward the satellite, and green-yellow values indicate detected stable areas. **B** Cross-sectional schematic illustrating the geometric relationship between the satellite, the tailings dam, and the PS points. The small red arrow from the InSAR data point indicates the direction of LOS movement, in this case away from the satellite. **C** Average cumulative LOS displacement time-series for the selected data points

as a single pixel may cover a significant part of the tailings dam being studied. A potential solution to this is TerraSAR-X for which the spatial resolution can be 1–3 m depending on the imaging mode. To our knowledge, only Holden et al. (2020) have conducted a comparison between the two satellites for a TSF failure (Feijao), whereas Gama et al. (2022) and a few studies in other sectors (e.g., Bischoff et al. 2017; Colombo 2021; Wang et al. 2021) have commented on the higher point density and lower standard deviation offered by TerraSAR-X. As such, Sentinel-1 appears to be more appropriate for monitoring larger-scale hazards.

The positional accuracy of observation points can also vary depending on the satellite. Although the precision of displacement measurements is millimetric, the position of observation points is known with a meter-scale accuracy. According to general insights from SqueeSAR case studies, the approximate point-elevation accuracy is ± 1.5 m for TerraSAR-X compared to ± 8 m for Sentinel-1. Furthermore, the approximate north–south and east–west point-location accuracy is ± 1 m and ± 3 m, respectively, for TerraSAR-X, compared to ± 8 m and ± 12 m for Sentinel-1. These differences are particularly important considerations when monitoring smaller-sized TSFs.

To overcome the limitations of C-band InSAR (e.g., Sentinel-1), the use of L-band data (e.g., ALOS PALSAR-1/2 and SAOCOM-1) could be more effective when monitoring TSFs in forested/wooded terrains due to the higher signal wavelengths of ~ 24 cm. An example of the application of L-band data for TSF monitoring is presented in Hu et al. (2017). The L-band and S-band (~ 12 cm wavelength) satellite NISAR is planned to be launched in 2024 with near-global coverage and a revisit interval of 12 days. Like Sentinel-1, the NISAR data will be made freely available. This will expand the scope and capabilities of InSAR monitoring

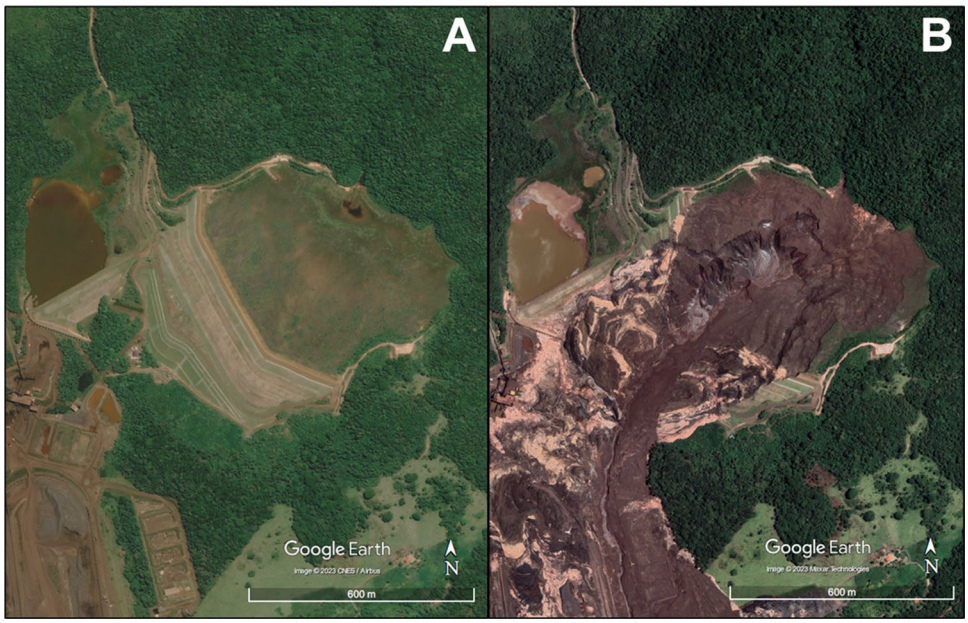


**Fig. 10** **A** Pre-failure (early January 2019) and **B** post-failure (early February 2019) Google Earth Worldview-2 (0.5 m resolution) images of the 25 January 2019 Feijao tailings dam breach in Brazil

of TSFs in diverse environmental settings and will enable case-study applications of multi-band InSAR data.

### Selection of processing software/algorithm

Each InSAR data processing software is founded on algorithms that filter and convert raw radar satellite data into point-cloud displacement data. The strengths and limitations of these algorithms differ depending on each software. To our knowledge, the present study is the first to directly compare different processing algorithms for a TSF site. The commercial SARScape Analytics package allows automated data processing and enables faster runtimes, thus making it convenient for multi-site, regional-scale assessments or comprehensive case study investigations. However, the automated approach also prevents the user from checking interferogram quality, modifying filtering techniques, or assigning/locating the reference point—a critical parameter for InSAR processing. These limitations generally do not exist in advanced commercial software (e.g., the complete SARScape package) and proprietary algorithms (e.g., SqueeSAR).

The ground-truth application showed a major difference in the performances of SARScape Analytics in comparison to SqueeSAR. In SqueeSAR, the number of data points increases with greater coherence, which contrasts with the statistical distribution for SARScape Analytics. This may reflect the different data filtering techniques in both algorithms, and it resulted in a much greater point density for SqueeSAR over the TSF. Moreover, the Tonglvshan case highlighted the issue of loss of coherence in SARScape Analytics that led to only a single data point along the breach section of the dam.

It appears that errors were manifested in the final two data points of the time-series for Cadia. This issue was not encountered in Carla et al. (2019a), who used SqueeSAR, nor in Jefferies et al. (2019), who implemented SBAS in the complete SARScape package. However, in Bayaraa et al (2022), the InSAR results that were processed using TerraMotion's ISBAS algorithm were characterized by notable variability and with significant deviations from the finite-element modeled deformations. The authors attributed this to the exceedance of the maximum measurable deformation of Sentinel-1 InSAR (28 mm over a 12-day revisit time) in the tertiary deformation phase, and it is likely that these issues impacted our results as well. Jefferies et al. (2019) also stated that SBAS is more appropriate for capturing non-linear accelerating movements compared to PS.

Lastly, a key judgment that influenced our InSAR data processing and the time-series analysis was our selection of the minimum coherence threshold: 0.70 for 3 sites, 0.65 for 1 site, and 0.57 for 1 site. The selections depended on the quality of InSAR data over the site and the need to filter out noise and obtain reliable time-series data. As stated in "Background and approach", our coherence thresholds were greater than the 0.45 value applied in the ISBAS analysis by Grebby et al. (2021) and comparable to the 0.60 value selected in the PS analysis by Mazzanti et al. (2021). The average coherence of InSAR data ultimately depends on the environmental conditions and the choice of processing algorithm (e.g., PS or SBAS or PS + DS)—an example of which is demonstrated in the ground-truth case. It is worth noting that technical guidance on appropriate coherence thresholds is rather limited, particularly for InSAR applications to mine areas.

## Implications for monitoring

### Accuracy

In the ground-truth assessment, we observed that both processing software/algorithms were able to represent the deformation regime of 0–50 mm/year on a site-scale, both on the tailings dam crest and the downstream slope. The RMSE between the InSAR and MP data was calculated to be up to 7 mm. The SARScape Analytics results had a slightly higher standard deviation (3.6 mm) compared to SqueeSAR (3.0 mm). However, the loss of data points along the embankment due to on-site activity prevented additional time-series comparisons.

This study highlights the complementary role that satellite InSAR can play in long-term monitoring programs at TSF sites. InSAR can be a valuable "hazard-screening" tool for active mines containing multiple TSFs or a large TSF, for monitoring inactive or closed TSFs, or for monitoring legacy/abandoned TSFs where installing and maintaining in-situ instrumentation can pose practical challenges. However, some precautionary notes are as follows:

- 1-D InSAR results often do not represent the maximum rate of movement that the dam is actually experiencing, nor does the LOS represent the true 3-D direction toward which the maximum rate of movement is occurring. This is a situation where the availability of satellite data of overlapping orbits can be important in retrieving 2-D displacements (vertical and east–west horizontal), which was not possible for any of our case studies.
- As stated earlier, sub-horizontal movements in the north–south direction tend to be poorly captured and potentially underestimated, due to the polar orbits of SAR satellites.
- On-site mining activities (e.g., construction, dam raise, tailings deposition, drilling) can lead to loss of InSAR data in an active TSF and may produce InSAR data patterns that can be potentially misinterpreted without sufficient site-specific knowledge.
- Routinely conducting ground-truth assessments with the support of in-situ data (e.g., geodetic, survey, instrumentation) provides value by verifying that the InSAR results are representative on a site-scale.

### Prediction of instability (location and timing)

When attempting to predict TSF instability using InSAR, there are two components that require attention: breach location and breach timing. Our study suggests that the breach location is generally easier to predict than the failure date. When using proprietary algorithms such as SqueeSAR, it appears that time-of-failure prediction capabilities are enhanced, given that the issues encountered with Cadia when using SARScape Analytics in this study were not observed in Carla et al. (2019a).

In the cases of Tonglvshan and Hindalco, there were other hotspots of detected movements in addition to the breach location. Given that these case studies were founded on relatively poor background knowledge, explaining why the breach occurred where it did was challenging using InSAR data alone.

Feijao is an interesting case where several studies (including the present) have conducted forensic InSAR investigations using different processing algorithms and have obtained reasonably similar rates of precursor deformation, yet have arrived at different conclusions on whether the failure timing was foreseeable. This is because, in certain sections of the dam, the precursor deformation patterns indicated minor accelerations which were subject to user-specific judgment, unlike the Cadia case that exhibited anomalous accelerations in the 3 months preceding the breach.

A key lesson to draw here is that, from a geotechnical perspective, not all failure modes can be expected to exhibit obvious, InSAR-detectable signs of precursor distress for weeks prior to dam collapse. While foundation instabilities may involve sequential phases of creep movement and acceleration under high loading conditions, internal erosion (piping) and seepage is a process that cannot be reliably detected via InSAR. Previous studies have also reported that some TSF failure mechanisms are onset without advance warning, either due to brittle collapse of the tailings structure (e.g., Feijao; Robertson et al. 2019) or sudden anthropogenic disturbances or localized triggers (Rana et al. 2021).

This is an important lesson for an engineer having to make decisions in real time based on InSAR data alone, without foreknowledge of the future failure. The main issue is that the satellite revisit interval remains too infrequent (6–12 days) for InSAR to be able to help identify the triggering mechanism or to capture the deformation behavior in the hours preceding a breach. This underscores the value of keeping continuous, accessible records of in-situ data and highlights why InSAR is a useful hazard-screening technology that can complement, but not substitute, on-the-ground observations. It is also worth acknowledging that the benefit of hindsight is an important factor in how the pre-failure InSAR data has been perceived in some forensic case studies, including the ones presented here.

## Study limitations

This study significantly improves InSAR case history knowledge for tailings dams, thus addressing a critical research gap for practitioners. However, the insights presented herein are conditioned by certain limitations that underpin the adopted approach. We briefly acknowledge the most important limitations below, and we refer to "Practical considerations" and

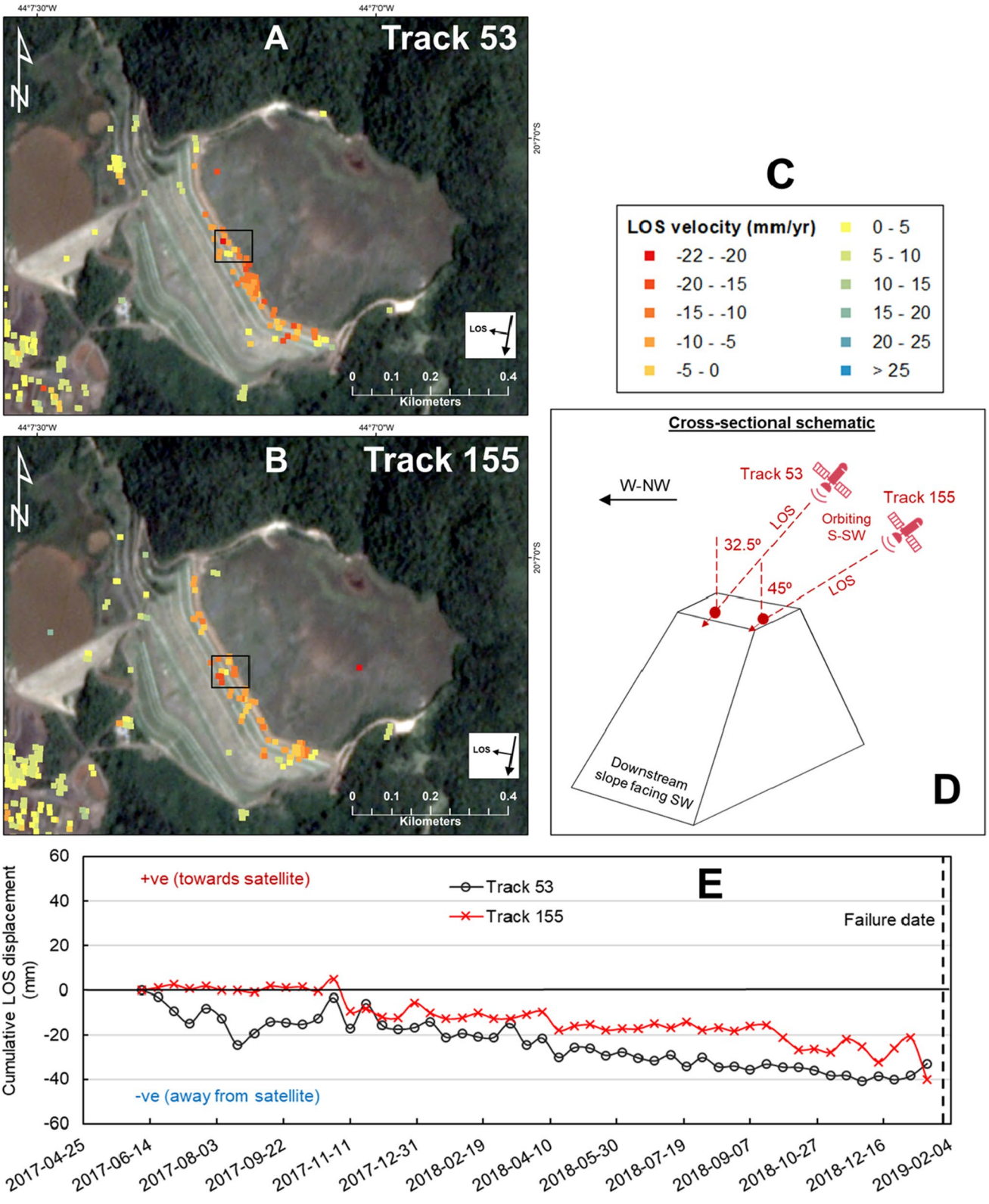
A
Track 53
B
Track 155
44°7'30"W
44°7'0"W
20°7'0"S
N
LOS
0 0.1 0.2 0.4
Kilometers
C
LOS velocity (mm/yr)
-22 - -20
-20 - -15
-15 - -10
-10 - -5
-5 - 0
0 - 5
5 - 10
10 - 15
15 - 20
20 - 25
> 25
Cross-sectional schematic
W-NW
Track 53
Track 155
Orbiting S-SW
LOS
32.5°
45°
Downstream slope facing SW
D
E
Cumulative LOS displacement (mm)
+ve (towards satellite)
-ve (away from satellite)
Track 53
Track 155
Failure date
60
40
20
0
-20
-40
-60
2017-04-25
2017-06-14
2017-08-03
2017-09-22
2017-11-11
2017-12-31
2018-02-19
2018-04-10
2018-05-30
2018-07-19
2018-09-07
2018-10-27
2018-12-16
2019-02-04

◂**Fig. 11** Sentinel-1 PS-InSAR results, processed on SARScape Analytics with a minimum coherence threshold of 0.70, for 2 satellite orbit tracks over the site of the 25 January 2019 Feijao TSF failure in Brazil. **A**, **B** Line-of-sight (LOS) velocity map for Track 53 and Track 155, annotated with the data points selected for time-series analysis. Negative (red) values indicate detected movements away from the satellite, positive (blue) values indicate detected movements toward the satellite, and green-yellow values indicate detected stable areas. **C** Legend of the LOS velocity maps. **D** Cross-sectional schematic illustrating the geometric relationship between the satellites, the dam, and the PS points selected for time-series analysis. The small red arrows indicate the direction of LOS displacement, in this case away from the satellite. **E** Cumulative LOS displacement time-series for the selected data points from Track 53 and Track 155

"Implications for monitoring" where the basis and implications of these limitations were discussed in greater detail:

1. *Selection of the SARScape Analytics processing software*. This included issues related to (i) the inability to assign or locate the reference point, (ii) errors when capturing tertiary-phase, rapid accelerations for Cadia, which were not encountered in previous studies, and (iii) the sole use of the PS technique for InSAR processing without comparison to the SBAS algorithm, which is more appropriate for monitoring vegetated areas and, according to Jefferies et al. (2019), for capturing accelerating movements.
2. *Selection of the minimum coherence threshold.* There is limited technical guidance on appropriate coherence thresholds for InSAR data processing over mine areas. We adopted best judgment based on previous studies (e.g., Grebby et al. 2021; Mazzanti et al. 2021) and applied a relatively high, strict coherence threshold to filter out noise and visualize and analyze reliable time-series data.
3. *No comparisons between Sentinel-1 and other forms of satellite data*. Such comparisons would have produced key insights into how different spatial resolutions and different signal wavelength bands influence InSAR data quality and accuracy for tailings dams in diverse site conditions.

## Concluding remarks

This study explored the capabilities and limitations of satellite InSAR to monitor the geotechnical stability of tailings dams. This research is timely considering the increased reliance on remote sensing for geotechnical monitoring in the tailings management industry and the need for more case study applications to enhance technical knowledge of InSAR. The goal of this study was to generate practical insights and considerations chiefly from an engineer's perspective. We used open-source, medium-resolution Sentinel-1 data to undertake a ground-truth assessment at a test site equipped with monitoring prism data and to conduct a forensic analysis of 5 failure cases. The methodology involved the use of a commercial software with an automated PS workflow (SARScape Analytics) for the ground-truth site and 4 of 5 failure cases and an advanced proprietary algorithm (SqueeSAR) implemented with a dual PS + DS technique for the ground-truth site and 1 failure case.

Based on the ground-truth site which has exhibited displacement rates of 0–50 mm/year, we find that Sentinel-1


**Fig. 12** **A** Pre-failure (9 April 2019) and **B** post-failure (9 May 2019) satellite images of the 9 April 2019 Hindalco tailings dam breach in India. Image **A** is PlanetScope (3 m resolution) and image **B** is Google Earth Worldview-2 (0.5 m resolution)

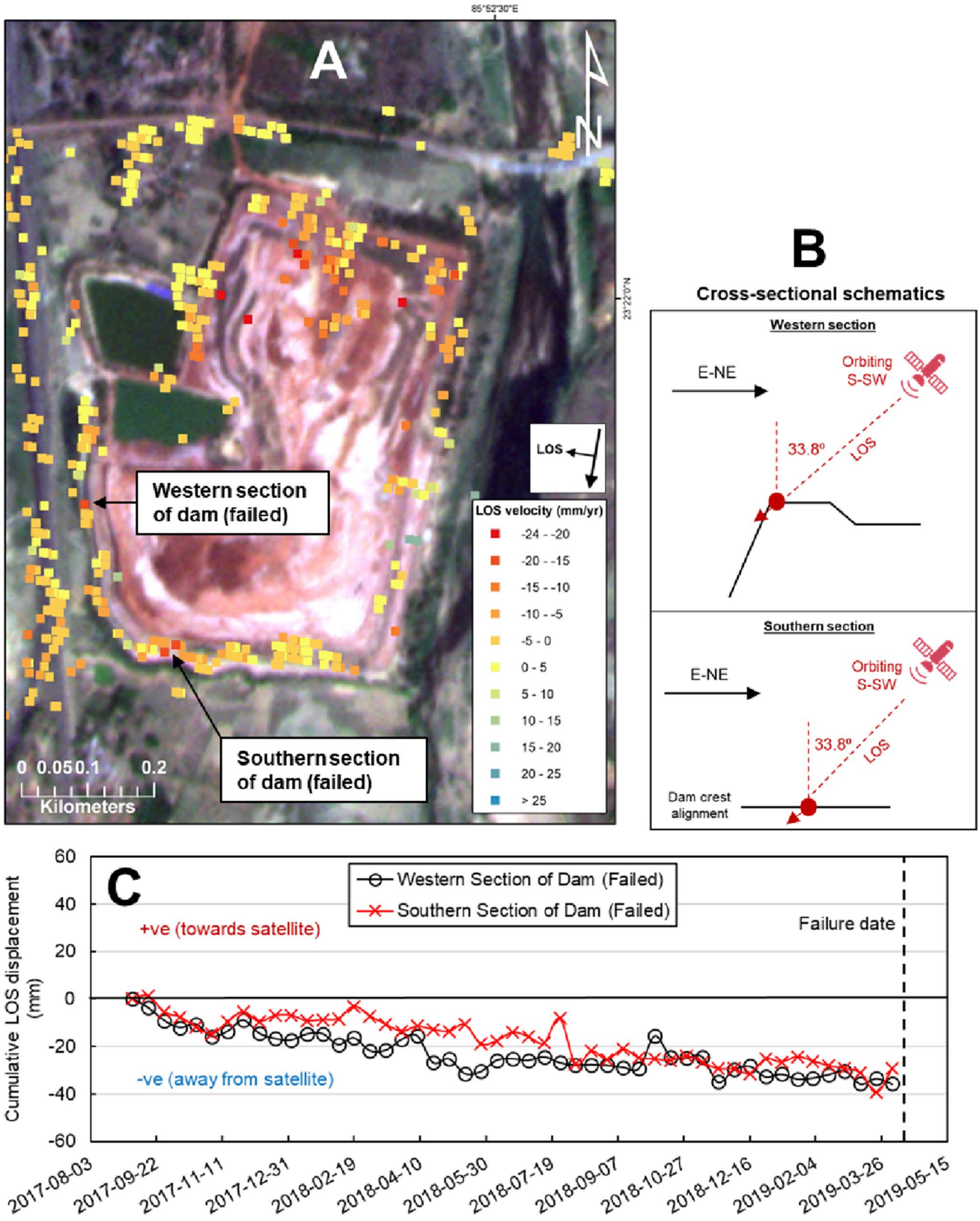
85°52'30"E
23°22'0"N
A
N
Western section of dam (failed)
Southern section of dam (failed)
LOS
LOS velocity (mm/yr)
-24 - -20
-20 - -15
-15 - -10
-10 - -5
-5 - 0
0 - 5
5 - 10
10 - 15
15 - 20
20 - 25
> 25
0 0.05 0.1 0.2
Kilometers
B
Cross-sectional schematics
Western section
E-NE
Orbiting S-SW
33.8°
LOS
Southern section
E-NE
Orbiting S-SW
33.8°
LOS
Dam crest alignment
C
Western Section of Dam (Failed)
Southern Section of Dam (Failed)
Failure date
+ve (towards satellite)
-ve (away from satellite)
Cumulative LOS displacement (mm)
60
40
20
0
-20
-40
-60
2017-08-03
2017-09-22
2017-11-11
2017-12-31
2018-02-19
2018-04-10
2018-05-30
2018-07-19
2018-09-07
2018-10-27
2018-12-16
2019-02-04
2019-03-26
2019-05-15

◂**Fig. 13** Sentinel-1 PS-InSAR results, processed on SARScape Analytics with a minimum coherence of 0.65, for the 9 April 2019 Hindalco TSF failure in India. **A** Line-of-sight (LOS) velocity map, annotated with the data points selected for time-series analysis. Negative (red) values indicate detected movements away from the satellite, positive (blue) values indicate detected movements toward the satellite, and green-yellow values indicate detected stable areas. **B** Cross-sectional schematics illustrating the geometric relationship between the satellite, the dam, and the PS points selected for time-series analysis. The small red arrows indicate the direction of detected LOS movement, in this case away from the satellite. **C** Cumulative LOS displacement time-series for the selected data points

InSAR can provide reasonable accuracy on a site-scale (for both the dam crest and downstream slope) with a maximum RMSE of 7 mm. In comparison to SARScape Analytics, SqueeSAR was shown to generate a greater point density and a higher average coherence.

Based on all of our forensic case studies, we conclude that Sentinel-1 InSAR can serve as a valuable hazard-screening tool in active mines with large TSFs or multiple TSFs, in mines with inactive or closed TSFs, and in legacy mines with abandoned TSFs, as it may help guide where to undertake targeted investigations. However, the benefit of hindsight is an important factor in how pre-failure InSAR data has been perceived in forensic case studies, including the ones presented herein. From a geotechnical hazard perspective, most potential failure modes associated with tailings dams may not exhibit InSAR-detectable accelerations in precursor deformation trends that could assist with real-time, time-of-failure prediction. Furthermore, the revisit interval of SAR satellites prevents detection of instantaneous failure mechanisms.

As such, long-term monitoring programs for tailings dams should ideally be integrated with a combination of remote sensing and field instrumentation to best support engineering practice and judgment. This study contributes to this effort by providing considerations on how InSAR data quality over tailings dam sites may be influenced by algorithm/satellite selection, environmental conditions, site activity, coherence thresholds, and satellite-dam geometry. Future research to build on this work could involve additional case-study comparisons between different forms of satellite data and between different processing algorithms/software.

## Appendix

**Table 4** Time-lapse videos showing the evolution of the TSF failure sites until their breach events

| TSF failure case | Number of PlanetScope images | Timespan | Open-access URL link |
|---|---|---|---|
| 2017 Tonglvshan, China | N/A | N/A | N/A |
| 2018 Cadia, Australia | 120 | Sept 2016–Sept 2018 | https://www.planet.com/stories/cadia-tsf-evolution-and-breach-AZZeTRo4g |
| 2018 Cieneguita, Mexico | 60 | Jan 2017–July 2018 | https://www.planet.com/stories/cieneguita-mexico-tsf-evolution-and-collapse-snnoZ62Vg |
| 2019 Feijao, Brazil | 90 | June 2017–Feb 2019 | https://www.planet.com/stories/feijao-tsf-failure-_57SR6h4g |
| 2019 Hindalco, India | 120 | Sept 2017–Sept 2019 | https://www.planet.com/stories/hindalco-tsf-evolution-zM7Se32Vg |

**Acknowledgements** This research was carried out within the CanBreach project which comprises five industrial partners (Imperial Oil, Suncor Energy, BGC Engineering, Klohn Crippen Berger, and Golder Associates) and three Canadian research institutions (University of Waterloo, The University of British Columbia, and Queen's University). The authors acknowledge the guidance and feedback provided by Jeanine Engelbrecht (BGC Engineering), Scott Martens (Teck Resources), Gideon Steyl (ATC Williams), and Joanna Chen (WSP Golder) during the preparation of this study, and thank the anonymous peer-reviewers for their comments which improved the quality of this manuscript. The authors also acknowledge the support of NV5 Geospatial (formerly L3Harris Geospatial), Sarmap, and TRE Altamira for the InSAR processing software/algorithms used in this study.

**Funding** The first phase of the CanBreach project (2019–2023) was joint-funded by the listed industrial partners and a Collaborative Research and Development (CRD) grant (CRDPJ 533226–18) issued by the Natural Sciences and Engineering Research Council (NSERC) of Canada. The lead author (N. Rana) was supported by the Science Domestic Scholarship and the President's Scholarship awarded by the University of Waterloo, the Queen Elizabeth II Graduate Scholarship in Science and Technology awarded by the Ontario Provincial Government in Canada, and the Gary Salmon Memorial Scholarship awarded by the Canadian Dam Association.

## References


Arenas A, Reid D, Fanni R, Smith K, Fourie A (2023) Numerical assessment of drilling-induced static liquefaction triggering of Feijão Dam I. In: Proceedings of the 10th Numerical Methods in Geotechnical Engineering, June 26–28, London, United Kingdom

Arroyo M, Gens A (2021) Computational analyses of dam i failure at the corrego de feijao mine in brumadinho (Final Report). Investigation commissioned by federal public prosecutor's office and vale S.A. https://www.cimne.com/vnews/m2381/11447/cimne-delivers-the-final-technical-report-on-the-brumadinho-disaster-to-the-brazilian-prosecutors-office. Accessed 6 Oct 2021

Aswathi J, Binojkumar RB, Oommen T, Bouali EH, Sajinkumar KS (2022) InSAR as a tool for monitoring hydropower projects: a review. Energy Geosci 3(2):160–171. https://doi.org/10.1016/j.engeos.2021.12.007

Bakon M, Perissin D, Lazecky M, Papco J (2014) Infrastructure non-linear deformation monitoring via satellite radar interferometry. Procedia Tech 16:294–300. https://doi.org/10.1016/j.protcy.2014.10.095

Bayaraa M, Sheil B, Rossi C (2022) InSAR and numerical modelling for tailings dam monitoring – the Cadia failure case study. Géotechnique 1–19. https://doi.org/10.1680/jgeot.21.00399

Berardino P, Fornaro G, Lanari R, Sansosti E (2002) A new algorithm for surface deformation monitoring based on small baseline differential SAR interferograms. IEEE Trans Geosci Remote Sens 40(11):2375–2383. https://doi.org/10.1109/TGRS.2002.803792

Bischoff CA, Ferretti A, Novali F, Uttini A, Giannico C, Meloni F (2020) Nationwide deformation monitoring with SqueeSAR® using Sentinel-1 data. Proc Int Assoc Hydrol Sci 382:31–37. https://doi.org/10.5194/piahs-382-31-2020

Bischoff CA, Basilico M, Ferretti A, Molinaro D, Giannico C, Ghail RC, Mason PJ (2017) A comparison between TerraSAR-X and Sentinel-1 PSInSAR data for infrastructure monitoring in London, UK. GRSG 28th International Annual Conference "Applied Geological Remote Sensing"

Blight GE (2010) Geotechnical engineering for mine waste storage facilities. CRC Press, London

Carlà T, Intrieri E, Raspini F, Bardi F, Farina P, Ferretti A, Colombo D, Novali F, Casagli N (2019a) Perspectives on the prediction of catastrophic slope failures from satellite InSAR. Sci Rep 9(1):1–9. https://doi.org/10.1038/s41598-019-50792-y

Carlà T, Tofani V, Lombardi L, Raspini F, Bianchini S, Bertolo D, Thuegaz P, Casagli N (2019b) Combination of GNSS, satellite InSAR, and GBInSAR remote sensing monitoring to improve the understanding of a large landslide in high alpine environment. Geomorph 335:62–75. https://doi.org/10.1016/j.geomorph.2019.03.014

Casu F, Manzo M, Lanari R (2006) A quantitative assessment of the SBAS algorithm performance for surface deformation retrieval from DInSAR data. Remote Sens Environ 102(3–4):195–210. https://doi.org/10.1016/j.rse.2006.01.023

Chen, C W, Zebker, H A (2002) Phase unwrapping for large SAR interferograms: Statistical segmentation and generalized network models. IEEE Trans Geosci Remote Sens 40(8):1709–1719. https://doi.org/10.1109/TGRS.2002.802453

Colombo, D (2021) Why InSAR monitoring in mining should be "high resolution". https://www.linkedin.com/pulse/why-insar-monitoring-mining-should-high-resolution-davide-colombo/.Accessed 10 Nov 2022

Crosetto M, Monserrat O, Iglesias R, Crippa B (2010) Persistent scatterer interferometry: potential limits and initial C- and X-band comparison. Photogramm Eng Remote Sens 76:1061–1069

Crosetto M, Monserrat O, Cuevas-González M, Devanthéry N, Crippa B (2016) Persistent scatterer interferometry: a review. ISPRS J Photogramm Remote Sens 115:78–89. https://doi.org/10.1016/j.isprsjprs.2015.10.011

Devanthéry N, Crosetto M, Monserrat O, Cuevas-González M, Crippa B (2014) An approach to persistent scatterer interferometry. Remote Sens 6(7):6662–6679. https://doi.org/10.3390/rs6076662

Duan H, Li Y, Jiang H, Li Q, Jiang W, Tian Y, Zhang J (2023) Retrospective monitoring of slope failure event of tailings dam using InSAR time-series observations. Nat Haz 117(3):2375–2391. https://doi.org/10.1007/s11069-023-05946-7

Ferretti A, Prati C, Rocca F (2001) Permanent scatterers in SAR interferometry. IEEE Trans Geosci Remote Sens 39(1):8–20. https://doi.org/10.1109/36.898661

Ferretti A, Fumagalli A, Novali F, Prati C, Rocca F, Rucci A (2011) A new algorithm for processing interferometric data-stacks: SqueeSAR. IEEE Trans Geosci Remote Sens 49(9):3460–3470. https://doi.org/10.1109/TGRS.2011.2124465

Gama, F F, Cantone, A, Mura, J C (2022) Monitoring horizontal and vertical components of SAMARCO mine dikes deformations by DInSAR-SBAS using TerraSAR-X and sentinel-1 data. Mining 2(4):725–745. https://doi.org/10.3390/mining2040040

Gama F, Mura JC, Paradella W, de Oliveira CG (2020) Deformations prior to the brumadinho dam collapse revealed by Sentinel-1 InSAR data using SBAS and PSI techniques. Remote Sens 12(21):3664. https://doi.org/10.3390/rs12213664

Ghahramani N, Mitchell A, Rana NM, McDougall S, Evans SG, Take A (2020) Tailings-flow runout analysis: examining the applicability of a semi-physical area–volume relationship using a novel database. Nat Hazards Earth Syst Sci. https://doi.org/10.5194/nhess-2020-199

Global Tailings Review (2020) Global industry standard on tailings management. https://globaltailingsreview.org/. Accessed 1 Sept 2020

Grebby S, Sowter A, Gluyas J, Toll D, Gee D, Athab A, Girindran R (2021) Advanced analysis of satellite data reveals ground deformation precursors to the Brumadinho Tailings Dam collapse. Commun Earth Environ 2(1):1–9. https://doi.org/10.1038/s43247-020-00079-2

Holden D, Donegan S, Pon A (2020) Brumadinho dam InSAR study: analysis of TerraSAR-X, COSMO-SkyMed and Sentinel-1 images preceding the collapse. In: Dight P (ed) International symposium on slope stability in open pit mining and civil engineering, Proceedings, Australian Centre for Geomechanics, pp 293–306

Hrysiewicz A, Wang X, Holohan EP (2023) EZ-InSAR: an easy-to-use open-source toolbox for mapping ground surface deformation using satellite interferometric synthetic aperture radar. Earth Sci Inform 16:1929–1945. https://doi.org/10.1007/s12145-023-00973-1

Hu X, Oommen T, Lu Z, Wang T, Kim JW (2017) Consolidation settlement of Salt Lake County tailings impoundment revealed by time-series InSAR observations from multiple radar satellites. Remote Sens Environ 202:199–209. https://doi.org/10.1016/j.rse.2017.05.023

Hudson R, Sato S, Morin R, McParland, MA (2021) Comparison of sentinel-1 and Radarsat-2 data for monitoring of tailings storage facilities. In: 13th European Conference on Synthetic Aperture Radar, online, pp 1-6

Islam K, Murakami S (2021) Global-scale impact analysis of mine tailings dam failures: 1915–2020. Glob Environ Change 70:102361. https://doi.org/10.1016/j.gloenvcha.2021.102361

Jefferies M, Morgenstern NR, Van Zyl DV, Wates J (2019) Report on NTSF embankment failure. Investigation report commissioned by Cadia Valley Operations for Ashurst Australia. https://www.newcrest.com/sites/default/files/2019-10/190417_Report%20on%20NTSF%20Embankment%20Failure%20at%20Cadia%20for%20Ashurst.pdf. Accessed 17 Apr 2019

Kim J, Coe JA, Lu Z, Avdievitch NN, Hults CP (2022) Spaceborne InSAR mapping of landslides and subsidence in rapidly deglaciating terrain, Glacier Bay National Park and Preserve and vicinity, Alaska and British Columbia. Remote Sens Environ 281:113231. https://doi.org/10.1016/j.rse.2022.113231

Kumar RM (2019) Muri hindalco red mud blasting(2). https://www.youtube.com/watch?v=8K63D70b4CU&ab_channel=R.Mkumar. Accessed 10 Apr 2019

Mazzanti, P, Antonielli, B, Sciortino, A, Scancella, S, Bozzano, F (2021) Tracking deformation processes at the legnica glogow copper district (Poland) by Satellite InSAR - II: Żelazny Most Tailings Dam. Land 10(6):654. https://doi.org/10.3390/land10060654

Mirmazloumi SM, Wassie Y, Nava L, Cuevas-González M, Crosetto M, Monserrat O (2023) InSAR time series and LSTM model to support early warning detection tools of ground instabilities: mining site case studies. Bull Eng Geol Environ 82(10):374. https://doi.org/10.1007/s10064-023-03388-w

Morgenstern NR, Vick SG, Van Zyl D (2015) Report on mount polley tailings storage facility breach. In: Report of independent expert engineering investigation and review panel for the Government of british columbia and the williams lake and soda creek indian bands (Canada)

Morgenstern NR, Vick SG, Viotti CB, Watts BD (2016) Report on the immediate causes of the failure of the fundao dam. https://www.resolutionmineeis.us/sites/default/files/references/fundao-2016.pdf. Accessed 1 Dec 2019

Pawluszek-Filipiak K, Wielgocka N, Tondaś D, Borkowski A (2023) Monitoring nonlinear and fast deformation caused by underground mining exploitation using multi-temporal Sentinel-1 radar interferometry and corner reflectors: application, validation and processing obstacles. Int J Digital Earth 16(1):251–271

Perissin D, Wang Z, Wang T (2011) The SARPROZ InSAR tool for urban subsidence/manmade structure stability monitoring in China. In: 34th International Symposium on Remote Sensing of Environment, Proceedings, Sydney

Rana NM, Ghahramani N, Evans SG, McDougall S, Small A, Take WA (2021) Catastrophic mass flows resulting from tailings impoundment failures. Eng Geol 292:106262. https://doi.org/10.1016/j.enggeo.2021.106262

Rana, NM, Ghahramani N, Evans SG, Small A, Skermer N, McDougall S, Take WA (2022) Global magnitude-frequency statistics of the failures and impacts of large water-retention dams and mine tailings impoundments. Earth-Sci Rev 232:104144. https://doi.org/10.1016/j.earscirev.2022.104144

Raspini F, Caleca F, Del Soldato M, Festa D, Confuorto P, Bianchini S (2022) Review of satellite radar interferometry for subsidence analysis. Earth-Sci Rev 235:104239. https://doi.org/10.1016/j.earscirev.2022.104239

Robertson PK, de Melo L, Williams DJ, Wilson GW (2019) Report of the expert panel on the technical causes of the failure of Feijao Dam I. Investigation report commissioned by Vale S.A. http://www.b1technicalinvestigation.com/. Accessed 12 Dec 2019

Rotta LHS, Alcantara E, Park E, Negri RG, Lin YN, Bernardo N, Mendes TSG, Filho CRS (2020) The 2019 Brumadinho tailings dam collapse: possible cause and impacts of the worst human and environmental disaster in Brazil. Int J Appl Earth Obs Geoinf 90:102119. https://doi.org/10.1016/j.jag.2020.102119

Sowter A, Amat MBC, Cigna F, Marsh S, Athab A, Alshammari L (2016) Mexico City land subsidence in 2014–2015 with Sentinel-1 IW TOPS: results using the intermittent SBAS (ISBAS) technique. Int J Appl Earth Obs Geoinf 52:230–242. https://doi.org/10.1016/j.jag.2016.06.015

Su C, Mergili M, Rana NM, Zhang S, Dai C, Wang B, Han Y (2024) Failure analysis and flow dynamic modeling using a new slow-flow functionality: the 2022 Jiaokou (China) tailings dam breach. Landslides 21:379–391. https://doi.org/10.1007/s10346-023-02146-z

Thomas A, Edwards SJ, Engels J, McCormack H, Hopkins V, Holley R (2019) Earth observation data and satellite InSAR for the remote monitoring of tailings storage facilities: a case study of Cadia Mine, Australia. In: Paterson A, Fourie A, Reid D (eds) 22nd International Conference on Paste, Thickened and Filtered Tailings, Proceedings, Australia

Vick SG (1983) Planning, design, and analysis of tailings dams. John Wiley & Sons, New York

Wang L, Deng K, Zheng M (2020) Research on ground deformation monitoring method in mining areas using the probability integral model fusion D-InSAR, sub-band InSAR and offset-tracking. Int J Appl Earth Obs Geoinf 85:101981. https://doi.org/10.1016/j.jag.2019.101981

Wang Y, Bai Z, Zhang Y, Qin Y, Lin Y, Li Y, Shen W (2021) Using TerraSAR X-band and Sentinel-1 C-band SAR interferometry for deformation along Beijing-Tianjin intercity railway analysis. IEEE J Select Topics Appl Earth Obs Remote Sens 14:4832–4841. https://doi.org/10.1109/JSTARS.2021.3076244

Werner C, Wegmüller U, Strozzi T, Wiesmann A (2000) Gamma SAR and interferometric processing software. In: ERS-Envisat Symposium, Proceedings, Gothenburg

Yunjun Z, Fattahi H, Amelung F (2019) Small baseline InSAR time series analysis: unwrapping error correction and noise reduction. Comput Geosci 133:104331. https://doi.org/10.1016/j.cageo.2019.104331

Zhuang Y, Jin K, Cheng Q, Xing A, Luo H (2022) Experimental and numerical investigations of a catastrophic tailings dam break in Daye, Hubei China. Bull Eng Geol Environ 81(1):1–16. https://doi.org/10.1007/s10064-021-02491-0